Accepted manuscript

Published as: Redesign of polyene macrolide glycosylation: engineered biosynthesis of 19-(*O*)-perosaminyl-amphoteronolide B. Chem. Biol. (2010) 17, 174 – 182. DOI: 10.1016/j.chembiol.2010.01.007

Redesign of polyene macrolide glycosylation: engineered biosynthesis of 19-(*O*)-perosaminyl-amphoteronolide B

Running title: Redesign of amphotericin glycosylation

Eve Hutchinson[1], Barry Murphy[2], Terence Dunne[1], Ciaran Breen[1], Bernard Rawlings[2] and Patrick Caffrey[1]*

[1]School of Biomolecular and Biomedical Science and Centre for Synthesis and Chemical Biology, University College Dublin, Belfield, Dublin 4, Ireland.

[2]Department of Chemistry, University of Leicester, University Road, Leicester LE1 7RH, United Kingdom

*Corresponding author. E-mail: patrick.caffrey@ucd.ie

Telephone: +353 1 716 1396

FAX: + 353 1 716 1183

ABSTRACT

Most polyene macrolide antibiotics are glycosylated with mycosamine (3,6-dideoxy-3-aminomannose). In the amphotericin B producer, *Streptomyces nodosus*, mycosamine biosynthesis begins with AmphDIII-catalysed conversion of GDP-mannose to GDP-4-keto-6-deoxymannose. This is converted to GDP-3-keto-6-deoxymannose, which is transaminated to mycosamine by the AmphDII protein. The glycosyltransferase AmphDI transfers mycosamine to amphotericin aglycones (amphoteronolides). The aromatic heptaene perimycin is unusual among polyenes in that the sugar is perosamine (4,6-dideoxy-4-aminomannose), which is synthesised by direct transamination of GDP-4-keto-6-deoxymannose. Here we use the *Streptomyces aminophilus perDII* perosamine synthase and *perDI* perosaminyltransferase genes to engineer biosynthesis of perosaminyl-amphoteronolide B in *S. nodosus*. Efficient production required a hybrid glycosyltransferase containing an N-terminal region of AmphDI and a C-terminal region of PerDI. This work will assist efforts to generate glycorandomised amphoteronolides for drug discovery.

INTRODUCTION

Many therapeutic agents are derived from polyketide and peptide natural products that contain sugar residues (Weymouth-Wilson, 1997). There is considerable interest in manipulating the sugar moieties of these compounds in order to identify analogues with improved pharmacological properties. Genetic studies on producer organisms have given insights into deoxyhexose biosynthesis and provided glycosyltransferase (GT) catalysts for addition of alternative sugars to aglycones. This work has led to production of new compounds by genetic engineering of producer strains and by *in vitro* glycosylation techniques (Blanchard and Thorson, 2006; Thibodeaux et al., 2007; Salas and Mendez, 2007). These studies have now been extended to polyene macrolides, antifungal agents that are also active against parasites, enveloped viruses and prions (Zhang et al., 2008).

Most polyene antibiotics are glycosylated with mycosamine (3, 6-dideoxy-3-amino-D-mannose). The aromatic heptaene perimycin (Figure 1, **1**) is unusual in that it contains perosamine (4, 6-dideoxy-4-amino-D-mannose) (Pawlak et al., 1995). Perosamine also appears in the lipopolysaccharides of several Gram-negative pathogens and its biosynthesis has been reconstituted using enzymes from such organisms (Alberman and Piepersberg, 2001; Zhao et al., 2007). The pathway entails conversion of GDP-mannose to GDP-4-keto-6-deoxymannose followed by transamination (Figure 2). Genes involved in mycosamine biosynthesis have been identified in several polyene-producing streptomycetes (Caffrey et al., 2008). We have focused on *Streptomyces nodosus*, which produces the medically important amphotericin B (Figure 3, **2**) along with a cometabolite, amphotericin A (**3**). The current view of the mycosamine pathway in this organism is shown in Figure 2. The AmphDIII GDP-mannose dehydratase

catalyses formation of GDP-4-keto-6-deoxy mannose that is converted to GDP-3-keto-6-deoxymannose. A transamination catalysed by the AmphDII protein generates the final activated sugar, GDP-mycosamine. It is unclear how the 3–ketosugar intermediate is formed. No enzyme has yet been identified that might catalyse 3, 4-ketoisomerisation of GDP-4-keto-6-deoxymannose. In the course of biochemical studies on GDP-fucose biosynthesis, Sullivan and co-workers (1998) used *Escherichia coli* and human GDP-mannose 4, 6 dehydratases to generate GDP-4-keto-6-deoxymannose *in vitro*. They obtained NMR evidence for spontaneous conversion of this intermediate to GDP-3-keto-6-deoxymannose. Thus it is possible that this step in mycosamine biosynthesis is not enzyme-catalysed *in vivo*. Spontaneous 3, 4 ketoisomerisation has also been observed with dTDP-4-keto-6-deoxyglucose, a key intermediate in the biosynthesis of many deoxyhexoses (Naundorf and Klaffke, 1996). However, enzymes that catalyse this reaction have been discovered more recently (Pfoestl et al., 2003). A well-studied example is Tyl1a that operates in the mycaminose biosynthetic pathway in *Streptomyces fradiae*, the tylosin producer (Melançon et al., 2006). This catalyses interconversion of the 4- and 3- ketosugars via an enediol intermediate (Tello et al., 2008). Although Tyl1a has been extensively characterised, the effects of disruption of the *tyl1a* gene on tylosin glycosylation have not yet been investigated. Indeed, Schell and co-workers have demonstrated biosynthesis of mycaminose in an engineered strain of *Saccharopolyspora erythraea* that has no 3, 4 ketoisomerase (Schell et al., 2008). These considerations suggest that 3, 4 ketoisomerases may be important when it is necessary to divert an NDP-4-keto-6-deoxyhexose away from competing pathways, or when isomerisation is

accompanied by a switch in alcohol stereochemistry at C-4. Neither of these conditions applies in mycosamine biosynthesis.

The amphotericin aglycones are synthesised by a large modular polyketide synthase (PKS) (Caffrey et al., 2001). The initial products are 8-deoxy-16-descarboxyl-16-methyl-amphoteronolides A and B (**4** and **5**, Figure 3). The AmphN cytochrome P450 oxidises the C-16 methyl group to a carboxyl group to form 8-deoxyamphoteronolides A and B (**6** and **7**). These are mycosaminylated by AmphDI and C-8 hydroxylated by AmphL to give amphotericins A and B (**2** and **3**). Targeted inactivation of *amphN* gives glycosylated amphotericin analogues in which methyl groups replace the exocyclic carboxyl groups (Carmody et al., 2005). Deletion of both *amphDII* and *amphN* gave analogues **8** and **9** that lack exocyclic carboxyl groups and are glycosylated with a 6-deoxyhexose, presumably a shunt product that results from reduction of the 4-keto or the 3-ketosugar intermediate by an unknown enzyme. The stereochemistry has not yet been determined for C-3 and C-4 of the reduced sugar. These results indicated that AmphDI might have some tolerance towards sugar and aglycone substrates. However, Zhang and co-workers (2008) carried out *in vitro* studies with hexahistidine-tagged forms of AmphDI and NysDI, the mycosaminyl transferase from the nystatin producer *Streptomyces noursei* (Nedal et al., 2007). Both enzymes were found to have narrow sugar substrate specificity, recognising only GDP-D-mannose and GDP-L-gulose out of a panel of 21 synthetic GDP-sugars (Zhang et al., 2008). GDP-perosamine was not investigated in this study.

Crystal structures have been determined for several plant and bacterial GTs that act on bioactive natural products (Truman et al., 2009). Despite this progress, only a few

of these enzymes have been successfully redesigned. Sugar and aglycone substrate specificities have been altered by mutagenesis or by construction of hybrid enzymes. In an early landmark study, Hoffmeister and co-workers (2002) investigated extending glycosyltransferases UrdGT1c and UrdGT1b that incorporate rhodinose and olivose, respectively, as the second and third sugars in the linear trisaccharide chain of urdamycins. Ten amino acids were shown to determine donor and acceptor specificity. Mutagenesis of these residues gave a GT that formed urdamycin P, which has a branched trisaccharide chain. Another important example of a redesigned GT is OleD, which normally catalyses addition of a glucosyl residue to C2″ of the desosamine sugar of oleandomycin. Thorson and co-workers carried out high throughput screening to identify four key mutations that increase a weak activity towards small aromatic acceptors (Williams et al., 2007). Saturation mutagenesis at three of these positions increased tolerance towards NDP-sugar donors as well as acceptors (Williams et al., 2008a; Williams et al., 2008b). Domain swapping can give a predictable switch in GT substrate specificity. This method has recently been used to construct hybrid GTs that transfer alternative sugars onto deoxystreptamine (Park et al., 2009), and glycopeptide acceptors (Truman et al., 2009). The approach has also expanded the range of flavonoid acceptors used by plant UDP-glucosyltransferases (Hansen et al., 2009). However, many hybrids are non-functional, possibly because artificially fused NDP-sugar- and acceptor-binding domains may fail to engage in interactions that are necessary for overall activity.

All of the GT engineering that has been carried out so far has been done with enzymes that use dTDP- or UDP-linked sugars. PerDI and AmphDI use GDP-perosamine and GDP-mycosamine respectively and are not closely related to any natural

product GTs that have been redesigned or structurally characterised. Here we undertake the first *in vivo* glycosylation engineering of amphotericin B. The genes for perosamine biosynthesis and attachment were cloned from the perimycin producer *Streptomyces aminophilus*. The PerDI perosaminyl transferase is of interest because it transfers a sugar other than mycosamine to a polyene macrolactone. In principle, introduction of the *perDII* perosamine synthase gene into *S. nodosus* should result in biosynthesis of GDP-perosamine. We aimed to investigate whether AmphDI, PerDI or engineered GTs could synthesise perosaminyl-amphoteronolides. These studies should assist further attempts to engineer the biosynthesis of amphotericin analogues with altered sugar residues.

RESULTS

Cloning of perimycin biosynthetic genes

A cosmid library was constructed from genomic DNA of *S. aminophilus*. The library was screened with DNA probes derived from amphotericin PKS genes. Hybridising cosmids were isolated and restriction fragments were subcloned into pUC118 for limited sequencing. Sequences from the ends of cosmid inserts were used to design oligonucleotide primers so that overlapping clones could be identified by PCR. This approach was used to assemble a set of cosmids representing the entire cluster. The partial sequencing indicated that the organisation of genes is similar to that in the candicidin/FR008 cluster (Chen et al., 2003). Homologues of polyene glycosyltransferase and sugar aminotransferase genes were found at one end of the cluster. Complete sequencing of a 4919 bp region (Genbank accession number = GQ380697) revealed *perDI* and *perDII* genes for perosaminyltransferase and perosamine synthase. In the sequenced region, the *perDI* gene was preceded by part of an *N*-methylase gene whereas *perDII* was followed by a discrete thioesterase (TE) gene and the 5′ end of a *p*-aminobenzoic acid synthase (PABA) gene. *N*-Methylase and PABA synthase enzymes are required for synthesis of the starter unit of the perimycin polyketide. In *Streptomyces* sp FR008, the region immediately downstream from the *fscMII* mycosamine synthase gene contains genes for a cytochrome P450 and ferredoxin that catalyse formation of the exocyclic carboxyl group in FR008/candicidin. This late modification does not occur in perimycin biosynthesis and the region between *perDII* and the discrete TE gene consists of 76 bp of non-coding DNA.

PerDI shows 63 to 72% sequence identity with mycosaminyl transferases whereas PerDII shows 73 to 77 % sequence identity with mycosamine synthases (Supplementary figure S1). Some of the differences between PerDII and mycosamine synthases correspond to positions that have been identified as active site residues in perosamine synthases from other bacteria (Cook and Holden, 2008).

The *perDIII* gene for GDP-mannose 4, 6 dehydratase was found at the opposite end of the cluster. Sequencing of a 3627 bp region (accession number = GQ380698) revealed that PerDIII shows 76 to 81% sequence identity with GDP-mannose dehydratases that function in GDP-mycosamine biosynthesis (Supplementary figure S1). The upstream region contained a gene for a β-glucosidase with strong homology to cellobiose hydrolases. This gene probably marks the end of the cluster because it has no obvious role in perimycin biosynthesis. The downstream DNA contained a 553 bp stretch homologous to the 5′ end of *fscD*, which encodes modules 11 to 16 of the FR008/candicidin PKS. Since our main interest was in perosamine synthesis and attachment, the remainder of the perimycin cluster was not sequenced at this stage.

Inactivation of *amphDII*

Previous work had generated a Δ*amphDII-NM* mutant that produced 16-descarboxyl-16-methyl-19-*O*-deoxyhexosyl amphoteronolide B (**8**) and a tetraene analogue (**9**) that is not C-8 hydroxylated (Carmody et al., 2005). This mutant retained a thiostrepton resistance (*tsr*) gene embedded in the chromosome. In this study, it was necessary to generate thiostrepton-sensitive Δ*amphDII* mutants that could be transformed with plasmid constructs that have *tsr* as a selectable marker. A frameshift mutation was

introduced into a cloned copy of the *amphDII* gene by end-filling an internal NcoI site (nucleotides 63698 – 63703, accession AF357202). A StuI-PstI fragment (nucleotides 62661 – 65543) containing the mutated *amphDII* sequence was cloned into KC-UCD1 (Carmody et al., 2004). The resulting phage was used to replace the *amphDII* gene in wild type *S. nodosus* and in the Δ*amphNM* mutant. The genotypes of the resulting Δ*amphDII* and Δ*amphDII-NM* mutants were verified by PCR (Figure 4).

S. nodosus Δ*amphDII* produced polyenes with masses consistent with 6-deoxyhexosyl-amphoteronolide B (**10**), aglycones 8-deoxyamphoteronolides A (**5**) and B (**6**) and amphoteronolide B (Supplementary Figure S2). The mixture had no detectable antifungal activity at total polyene concentrations as high as 50 μg/ml. This was consistent with absence of the amino sugar. The fact that all polyenes produced by this strain had exocyclic carboxyl groups indicates that the frameshift mutation in *amphDII* does not affect expression of the downstream *amphN* cytochrome p450 gene. *S. nodosus* Δ*amphDII-NM* produced 6-deoxyhexosylated polyenes lacking exocyclic carboxyl groups (**8** and **9**) detected previously by Carmody et al., (2005) as well as aglycones 8-deoxy-16-descarboxyl-16-methyl-amphoteronolides A and B (**4** and **5**).

The *amphDII* gene was amplified and cloned into the expression vector pIAGO (Aguirrezabalaga et al., 2000) under the control of the *ermE* promoter. The resulting pIAGO-*amphDII* construct was transformed into *S. nodosus* Δ*amphDII* and *S. nodosus* Δ*amphDII-NM*. The plasmid-borne *amphDII* gene restored efficient production of active mycosaminylated amphotericins in both strains (not shown).

Attempts to engineer the biosynthesis of perosaminyl-amphoteronolides

Previous inactivation of the *amphDIII* gene gave a mutant that synthesised 8-deoxyamphoteronolide A (**7**) as a major product (Byrne et al., 2003). The *perDIII* gene was cloned into pIAGO and transformed into *S. nodosus* Δ*amphDIII*. Analysis of polyene extracts revealed that the resulting transformant produced a mixture of aglycone **7** and glycosylated amphotericins **2** and **3** in approximately equal amounts (not shown) whereas the host containing the empty vector synthesised aglycone **7** only. The fact that PerDIII can substitute for AmphDIII is consistent with the proposed mycosamine biosynthetic pathway shown in Figure 2. In *S. nodosus*, the PerDII protein should be able to intercept GDP-4-keto-4, 6-dideoxymannose, produced by AmphDIII, and catalyse formation of GDP-perosamine.

We first attempted to replace the *S. nodosus* chromosomal *amphDI-DII* genes with *perDI-DII* genes. This was expected to reveal whether or not PerDI could transfer perosamine onto amphotericin aglycones. A recombinant phage was constructed to contain the *perDI-DII* genes flanked by sequences upstream and downstream of the *amphDI-DII-NM* region. The *perDI* start codon was precisely located downstream from the *amphDI* promoter and ribosome-binding site. Attempts to carry out the gene replacement in *S. nodosus* ΔNM yielded a deletion mutant lacking *amphDI-DII-NM* and containing *perDI-DII* (Supplementary Figure S3), which had the required genotype. This strain produced low levels of aglycones **4** and **5** but no glycosylated forms (Figure S4). This provided evidence that PerDI does not recognize amphoteronolides lacking exocyclic carboxyl groups, even though these aglycones resemble its natural substrate

around the glycosylation site. Attempts to obtain a perfect replacement of *amphDI-DII* by *perDI-DII* were therefore discontinued.

The 8-deoxy-16-descarboxyl-16-methyl amphoteronolide B product (**4**) had a lower methanol-solubility than other amphoteronolides and precipitated selectively on partial concentration of crude methanol extracts. It could be purified in 100 mg quantities from strains containing mutations in Δ*amphNM* and glycosylation genes. Structural analysis of this material by NMR will be described elsewhere. This aglycone may be useful for *in vitro* studies on polyene glycosylation and exocyclic carboxyl group formation.

The pIAGO-*perDII* plasmid was introduced into *S. nodosus* Δ*amphDII*. Crude polyenes extracted from this transformant showed a low level of antifungal activity. Analysis of the polyene mixture by HPLC revealed a low level of a new polyene, in addition to those produced by the host strain containing the empty vector, 8-deoxyamphoteronolide B (**6**) and 6-deoxyhexosyl-amphoteronolide B (**8**) (Figure 5, A and B). The new compound was a minor component and made up 2% of the total polyene. Further analysis revealed that this compound had a mass appropriate for **11**. The yield of this product was too low to allow further purification and analysis. This result suggested that AmphDI can perosaminylate amphoteronolides, but very inefficiently. The fact that the deoxyhexosylated analogue **8** remained as the major product suggests that AmphDI has a preference for GDP-deoxyhexose over GDP-perosamine. Overproduction of AmphDI was not expected to change the proportions of polyene products or to increase the yield of **11**. Attempts were therefore made to construct a hybrid GT.

Assessment of AmphDI-PerDI hybrid GTs

The GTs involved in natural product glycosylation belong to the GT-B superfamily and have N-terminal and C-terminal domains that function in recognition of acceptor and NDP-sugar donor substrates, respectively. In an effort to increase the yield of the putative perosaminylated analogue, hybrid GTs were constructed in which the putative 8-deoxyamphoteronolide-binding N-terminal domain of AmphDI was fused to the putative GDP-perosamine-binding C-terminal domain of PerDI. The internal boundaries of these substrate-binding domains were uncertain since PerDI and the mycosaminyl transferases are not closely related to natural product GTs that have been characterised more extensively (Liang and Qiao, 2007). It was therefore necessary to identify a functional cross-over point by trial and error. Two hybrid genes were made in initial attempts to design a GT that could efficiently modify the amphotericin aglycone with perosamine. To construct the first of these, the OGTF and GTR1 primers were used to amplify the 5′ region of the *amphDI* gene from the ribosome-binding site to the codons for E191-L192. The GTF1 and OGTR primers were used to amplify the *S. aminophilus* DNA region from the corresponding *perDI* codons for E191-L192 to the end of *perDII*. In both AmphDI and PerDI, E191-L192 are encoded by GAG-CTG codons. In each case the second codon was altered so as to create a SacI site (GAGCTC). The two products were ligated through their SacI sites to create a hybrid *amphDI-perDI* gene (*hap1*) linked to a *perDII* gene. This DNA was cloned between the BamHI and HindIII sites of pIAGO to form pIAGO-*hap1*.

The second hybrid GT gene (*hap2*) was constructed using primer pairs OGTF plus GTR3 and GTF3 plus OGTR. In this case the two products were joined through a

SacI site introduced to represent GAG-CTC codons for E246-L247 of AmphDI and E244-L245 of PerDI. The second construct was named pIAGO-*hap2*. The cross-over points in Hap1 and Hap2 are highlighted in Supplementary Figure S1A.

The pIAGO-*hap1* and pIAGO-*hap2* plasmids were introduced into the Δ*amphDII* and Δ*amphDII-NM* mutants. The two constructs differ at only 59 nucleotide positions in a central 165 bp stretch within the GT gene. Thus the expression levels of the two hybrid genes are expected to be similar. In the Δ*amphDII* strain, pIAGO-*hap1* had the same effect as pIAGO-*perDII* but pIAGO-*hap2* increased the yield of the new analogue (**11**) to approximately 25% of the total polyene, and brought about a corresponding decrease in the amount of the aglycone **6** (Figure 5C). This change was caused by the *hap2* gene because the strains are otherwise isogenic. In an additional control experiment, a pIAGO-*perDI-perDII* construct did not elevate production of the new polyene, confirming that PerDI does not recognise amphoteronolides even when expressed from the *ermE* promoter. These results show that Hap2 is a functional hybrid GT in which the amphoteronolide-binding domain of AmphDI has been grafted onto the GDP-perosamine-binding domain of PerDI. Although the two hybrid proteins differ by only 24 amino acids out of 460, Hap2 boosted production of **11** whereas Hap1 did not. This shows that the choice of cross-over point is critical. It should be noted that the pIAGO vector does not give particularly high expression of cloned genes in *S. nodosus*. None of the GTs (AmphDI, PerDI, Hap1, Hap2) could be detected as a prominent band when cell lysates of the various transformants were analysed by SDS-polyacrylamide gel electrophoresis.

The new compound had a retention time different to that of amphotericin B (Supplementary Figure S5). The mass was that expected for perosaminyl-amphoteronolide B (**11**) ($[M - H]^-$ = 922.5; $[M + Na]^+$ = 946.5) (Supplementary Figure S6). The yields of the new polyene from *S. nodosus* Δ*amphDII* pIAGO-*hap2* were typically around 40 mg/L. No perosaminylated tetraenes were observed.

Analysis of perosaminylated analogue by NMR

The analogue was purified and examined by proton and COSY NMR. Most resonances are similar to those found in amphotericin B (Supplementary Figures S7 and S8). The four methyl groups in amphotericin B show NMR resonances in d^6-DMSO as doublets at 0.91, 1.04, 1.11 and 1.13 ppm (McNamara et al., 1998), the last assigned to the mycosaminyl methyl group. NMR analysis of HPLC purified **11** (*ca*. 2 mg) in DMSO at 40^{o}C showed four methyl doublets at 0.93, 1.05, 1.13 and 1.17 ppm, this last value has moved downfield, and the resonance was considerably broadened. Addition of an equivalent of methanoic acid to the NMR sample sharpened this doublet, and moved it further downfield to 1.24 ppm, presumably due to the close proximity in space of the perosaminyl's equatorial protonated 4-amino group. The resonance at 2.81 ppm, assigned to the 4′-CH(NH_2) proton shows two large transdiaxial coupling constants of *ca*. 9.5 Hz to 3.37 ppm (5′) and 3.44 (3′). The 2′-proton at 3.70 ppm has a small axial/equatorial coupling constant of 2.7 Hz to the 3′-proton. The 1′-proton has moved from 4.61 in amphotericin B upfield to 4.35 ppm in the perosaminyl analogue. Reported NMR analysis of *N*-acetyl perimycin in deuterated pyridine/methanol has coupling

constants for 2′ of 0.0 and 3.0 Hz; those for 3′ are 3.0 and 10.0, and those for 4′ are 10.0 and 10.0 (Pawlak et al., 1995).

Perosaminylation of amphoteronolides lacking exocyclic carboxyl groups

The pIAGO-*hap2* plasmid was also introduced into the *S. nodosus* Δ*amphDII-NM* strain that produces aglycones lacking exocyclic carboxyl groups. This resulted in formation of a new minor polyene product not produced by the parent strain. Analysis by ESMS indicated that 16-descarboxyl-16-methyl-19-*O*-perosaminyl-amphoteronolide B (**12**) was produced ($[M + H]^+$ = 894.5; $[M – H_2O + H]^+$ = 876.5]; $[M + Na]^+$ = 916.5; formic acid adducts were detected in negative ion mode ($[M + HCOOH]^-$ = 938.5). It was not possible to purify this minor component in quantities sufficient for further analysis. However, it can be concluded that the Hap2 GT is capable of transferring perosaminyl residues to amphoteronolides lacking exocyclic carboxyl groups.

Biological activities of 19-*O*-perosaminyl-amphoteronolide B

Bioassays against *Saccharomyces cerevisiae* indicated that perosaminyl-amphoteronolide B had a minimal inhibitory concentration of 1.9 μg/ml. In parallel control assays, amphotericin B had an MIC of 2.1 μg/ml. The two polyenes also had approximately the same haemolytic activity. The polyene concentrations giving 50% haemolysis (MHC_{50} values) were 3.125 and 3.7 μg/ml for perosaminyl-amphoteronolide B and amphotericin B, respectively indicating similar potential toxicity. Thus replacing mycosamine with perosamine may have only a small overall positive effect on these

biological activities. However, the chromatographic properties of **11** show that it is slightly more water-soluble than amphotericin B.

DISCUSSION

Enzymatic glycorandomisation of polyene macrolides will require libraries of NDP-sugar donors and sugar-flexible GTs. Chemical and enzymatic methods have been developed for synthesis of NDP-sugars. These methods have already been used to synthesise 18 different GDP-sugars *in vitro*. Salas and co-workers have assembled plasmid constructs that direct intracellular synthesis of 12 different dTDP-deoxyhexoses (Mendez and Salas, 2007). A similar approach might be possible for *in vivo* generation of up to nine naturally occurring GDP-sugars (D-rhamnose, D-mannose, L-fucose, L-colitose, L-gulose, L-galactose, D-altrose, 6-deoxy-D-talose and L-fucofuranose). Prospects for generating unnatural NDP-sugars *in vivo* have also been discussed (Hui et al., 2007; Nic Lochlainn and Caffrey, 2009). While technologies for generating NDP-sugars are advanced, previous studies indicated that polyene GTs show limited tolerance towards these alternative substrates. This work takes the first step towards addressing this issue.

Here, our *in vivo* studies indicate that the PerDI perosaminyl transferase does not act on amphotericin aglycones and that the AmphDI mycosaminyl transferase inefficiently recognises GDP-perosamine. In the Δ*amphDII* strain containing pIAGO-*perDII*, AmphDI generated small amounts of perosaminyl-amphoteronolide B. This represents the first example of rational engineering of polyene macrolide glycosylation. Introduction of the Hap2 hybrid GT significantly increased the yield of perosaminyl-

amphoteronolide B. This shows that the aglycone-specificity of PerDI has been modified. To date, only a few natural product GTs have been re-designed successfully. To our knowledge, this is the first example involving a GT that acts directly on a complex polyketide macrolactone.

The activity of Hap2 indicates that the AmphDI region from residues 1 to 247 functions in aglycone recognition whereas the PerDI region from residues 248 to 458 is capable of binding GDP-perosamine. This finding is important because it should guide efforts to graft the amphoteronolide-binding domain onto C-terminal domains that recognize dTDP-glucose-derived deoxyhexoses. A greater array of these sugars is available. In addition, GDP-perosamine and GDP-mycosamine binding domains can be fused to N-terminal domains of GTs that recognize other natural product aglycones.

The *S. nodosus* Δ*amphDII* pIAGO-*hap2* transformant retains a functional *amphDI* gene and produces 6-deoxyhexosyl-amphoteronolide B as well as 19-*O*-perosaminyl-amphoteronolide B. Formation of the GDP-deoxyhexose apparently competes with GDP-perosamine biosynthesis in this strain. It is possible that GDP-4-keto-6-deoxymannose undergoes rapid 3, 4-ketoisomerisation and/or reduction. Sequence analysis of the *S. nodosus* genome may help to identify candidate genes for the 3,4 ketoisomerase, if it exists, and the reductase. This will allow deletion of pathways that divert GDP-4-keto-6-deoxymannose away from biosynthesis of alternative GDP-sugars.

Replacing the mycosamine of amphotericin B with perosamine made little difference to antifungal or haemolytic activity. This was not surprising, because previous chemical modification studies have shown that while a positive charge on the sugar residue is essential for antifungal activity of amphotericin B, its exact location is not

critical (Cheron et al., 1988). Recently, a *Streptomyces* species was identified that naturally produces an analogue of pimaricin in which mycosamine is replaced by perosamine (Komaki et al., 2009). The perosaminylated analogue had a 4-fold decrease in antifungal activity relative to pimaricin. The mode of action of pimaricin is different from that of other polyenes (te Welscher et al., 2008). This may explain why moving the sugar amino group has a greater impact on activity in the case of pimaricin. At neutral pH, amphotericin B exists as a zwitterion in which the positive charge on the amino sugar neutralises the negative charge on the exocyclic carboxyl group. With perosaminyl-amphoteronolide B, increased separation of these charges appears to improve water-solubility slightly.

Whilst the aminosugar of amphotericin B is important for antifungal activity, preliminary evidence suggests that it may not be essential for other biological effects such as antiprion activity (Soler et al., 2008). Some of these additional activities might be enhanced by glycosylation engineering. The work reported here will enable the potential of polyene macrolides to be expored more fully.

SIGNIFICANCE

The biosynthesis of 19-*O*-perosaminyl-amphoteronolide B is the first rational redesign of polyene glycosylation by genetic engineering of a producer micro-organism. Production of this compound in good yield suggests that sustainable fermentation methods will be able to deliver valuable glycoengineered analogues in quantities sufficient for clinical development. Polyene macrolide GTs and are not closely related to previously characterised GTs and use GDP-sugar donors rather than dTDP- or UDP-

linked sugars. The construction of an active AmphDI-PerDI hybrid shows that aglycone- and NDP-sugar-binding domains can be also exchanged between these polyene GTs. The C-terminal regions of these enzymes can now be targeted in attempts to increase sugar flexibility. This work will assist future attempts at glycodiversification of polyene macrolides and other natural products.

EXPERIMENTAL PROCEDURES

DNA methods

S. aminophilus DSM 40057 was obtained from DSMZ. Total cellular DNA was isolated as described by Hopwood et al. (1985). Chromosomal DNA was partially digested with Sau3A1 and fragments in the size range 30 to 40 kb were purified by sucrose density gradient centrifugation. These fragments were ligated to BamHI-cut pWE15 cosmid vector DNA and packaged into lambda phage particles using a Promega Packagene kit. The library was propagated on *E. coli* XL-Blue MR.

DNA probes were prepared from the amphotericin cluster. The insert from cosmid 4 containing the *amphC* sequence and the insert from cosmid 16 containing the *amphI* sequence were used as PKS probes. Fragments were purified by preparative agarose gel electrophoresis and labelled with digoxygenin-linked dUTP using a Boehringer Mannheim non-radioactive labelling kit. DNA labelling, colony hybridisation and Southern hybridisation were carried out according to the

manufacturer's instructions. Deep Vent DNA polymerase was used in PCRs. DNA sequencing and re-sequencing was carried out by MWG Biotech.

To construct pIAGO-*perDIII*, pIAGO-*perDII* and pIAGO-*amphDII*, the individual genes were amplified with the forward and reverse primers listed in Table 1. The PCR products were digested with BamHI-HindIII or BglII-HindIII and cloned between the BamHI and HindIII sites of the pIAGO expression plasmid. The pIAGO-*hap1* and pIAGO-*hap2* plasmids were constructed as described in the Results section.

The pIAGO-*perDI-DII* construct was assembled as follows. A plasmid subclone CBY was digested at an EcoRI site just upstream from the *perDI* start codon and ribosome binding site. The cohesive end was repaired with T4 DNA polymerase. Digestion with HindIII excised a fragment corresponding to nucleotides 484 – 4919 of the sequenced region (GenBank accession GQ380697). Ligation between the HindIII and end-repaired BamHI sites of pIAGO positioned the *perDI-DII* region downstream from the *ermE* promoter.

Protoplast transformations and gene replacements were carried out as described previously (Carmody et al., 2004; Power et al., 2008).

General polyene purification

Polyenes were purified and characterised as described previously (Power et al., 2008). Production cultures were grown in 2-litre flasks containing: 5 g fructose, 15 g dextrin (Corn, Type II, 15% soluble), 7.5 g soybean flour (Type I), 2.5g $CaCO_3$, 12.5 g Amberlite XAD16 resin, and 250 mL deionised water. Flasks were shaken at 120 rpm (32 mm gyrotary) 28°C, for 3 days. Polyenes were extracted from sedimented mycelia

and resin into methanol. Rotary evaporation was used to concentrate the methanol extract to an aqueous residue from which the polyenes precipitated. The precipitate was washed first with water and then with chloroform. Drying gave a yellow powder containing partially purified mixed polyenes.

Large-scale purification of 19-*O*-perosaminyl-amphoteronolide B (11)

The mycelia and beads from a 7L culture (twenty-eight flasks) were harvested by centrifugation (Sorvall GSA, 10,000 rpm 10 min, 4°C). The combined pellets were finely dispersed in 7L methanol and left to soak for 18 h. The suspension was centrifuged and the supernatant extract was retained. The resulting pellet was re-extracted with a further 7L methanol. Assay of the combined methanol extracts by UV spectrophotometry (Shimadzu 2401 PC) gave 880 mg heptaenes and 950 mg tetraenes i..*e*. 125 mg/L heptaenes, and 135 mg/L tetraenes. The extinction co-efficient (ε) for monomeric amphotericin B at 405 nm is $1.7 \times 10^5\ M^{-1}cm^{-1}$. For amphotericin A, ε is $0.78 \times 10^5\ M^{-1}cm^{-1}$ at 318 nm.

The total methanolic extract was concentrated *in vacuo* (below 40°C) until a yellow precipitate formed. This was harvested by centrifugation. The initial precipitate contained 750 mg heptaenes and 400 mg tetraenes. Washing with deionised water (2x50ml) gave 700 mg heptaenes and 100 mg tetraenes. After freeze drying the total dry weight of yellow powder was 1.2g.

Further purification was carried out on a Varian Prostar 210 diode array HPLC with 'Galaxieworkstation" software and UV Diode array detector. The columns (Supelco Ascentis) were: C8 reverse phase silica, 5 µm particle size, length 25 cm. The analytical

column had 4.6 mm diameter analytical column was run at a flow rate of 1 mL/min with sample volumes of 0.02 mL in methanol. A 21.2 mm diameter preparative column was run at a flow rate of 14.8 mL/min with a typical injection volume of 1.0 mL in DMSO. The solvent system was: water (A) and methanol containing 0.1% v/v formic acid (B). The gradients were typically 50 – 90% B over 28 minutes.

Polyene Analysis

Low resolution electrospray mass spectrometry was carried out on a triple Quadropole Micromass Quattro LC instrument. High resolution mass spectrometry was carried out using a Kratos Concept 1H double focussing high resolution sector instrument. FAB (Fast atom bombardment) spectroscopy was carried out using 3-nitrobenyl alcohol matrix with HRMS peak matching referenced to stable reference peaks.

NMR spectra were obtained using a Bruker AV500 MHz instrument. A sample of perosaminyl-amphoteronolide B (**11**) was purified twice by HPLC to obtain 2mg. This was dissolved in d6-DMSO and analysed at room temperature (298K) with the water peak suppressed.

Antifungal and haemolytic activities were assayed as described (Carmody et al., 2005).

ACKNOWLEDGEMENTS

PC received grants from the European Union (GENOVA QLRT-1999-00095) and from the Irish Higher Education Authority (PRTLI cycle 3). Some of the work in this

publication has emanated from research conducted with the financial support of Science Foundation Ireland under Grant Number 09/RFP/GEN2132. BJR received a grant from the BBSRC (BB/D017270/1).

REFERENCES

Aguirrezabalaga, I., Olano, C., Allende, N., Rodriguez, L., Brana, A. F., Mendez, C., and Salas, J. A. (2000). Identification and expression of genes involved in biosynthesis of L-oleandrose and its intermediate L-olivose in the oleandomycin producer *Streptomyces antibioticus*. Antimicrob. Agents Chemother. 44, 1266-1275.

Alberman, M., and Piepersberg, W. (2001). Expression and identification of the RfbE protein from *Vibrio cholerae* O1 and its use for the enzymatic synthesis of GDP-perosamine. Glycobiology 11(8), 655-661

Blanchard, S., and Thorson, J. S. (2006). Enzymatic tools for engineering natural product glycosylation. Current Opinion in Chemical Biology 10, 263-271

Byrne, B., Carmody, M., Gibson, E., Rawlings, B., and Caffrey, P. (2003). Biosynthesis of 8-deoxyamphotericins and 8-deoxyamphoteronolides by engineered strains of *Streptomyces nodosus*. Chem. Biol. 10, 1215-1224.

Caffrey, P., Lynch, S., Flood, E., Finnan, S., and Oliynyk, M. (2001). Amphotericin biosynthesis in *Streptomyces nodosus*: deductions from analysis of polyketide synthase and late genes. Chem. Biol. 8, 713 - 723.

Caffrey, P., Aparicio, J. F., Malpartida, F., and Zotchev, S. B. (2008). Biosynthetic engineering of polyene macrolides towards generation of improved antifungal and anitparasitic agents. Curr. Topics Med. Chem. 8, 639-653.

Carmody, M., Byrne, B., Murphy, B., Breen, C., Lynch, S., Flood, E., Finnan, S., and Caffrey, P. (2004). Analysis and manipulation of amphotericin biosynthetic genes by means of modified phage KC515 transduction techniques. Gene 343, 107-115.

Carmody, M., Murphy, B., Byrne, B., Power, P., Rai, D., Rawlings B., and Caffrey, P. (2005). Biosynthesis of amphotericin derivatives lacking exocyclic carboxyl groups. J. Biol. Chem. 280, 34420-34426.

Chen, S., Huang, X., Zhou, X., Bai, L., He, J., Jeong, K. J., Lee, S. Y., and Deng, Z. (2003). Organisational and mutational analysis of a complete FR-008/candicidin gene cluster encoding a structurally related polyene complex. Chem. Biol. 11, 357-366.

Cheron, M., Cybulska, B., Mazerski, J., Grzybowska, J., Czerwinski, A., and Borowski, E. (1988). Quantitative structure-activity relationships in amphotericin B derivatives. Biochem. Pharmacol. 37, 827 – 836.

Cook, P. D., Carney, A. E., and Holden, H. M. (2008). Accomodation of GDP-linked sugars in the active site of GDP-perosamine synthase. Biochemistry 47, 10685 -10693.

Hansen, E. H., Osmani, S. A., Kristensen, C., Moller, B. L., Hansen, J. (2009). Substrate specificities of family 1 UGTs gained by domain swapping. Phytochemistry 70, 473-482.

Hoffmeister, D., Wilkinson, B., Foster, G., Sidebottom, P. J., Ichinose, K., and Bechthold, A. (2002). Engineered urdamycin glycosyltransferases are broadened and altered in substrate specificity. Chem. Biol. 9, 287 – 295.

Hopwood, D. A., Bibb, M. J., Chater, K. F., Kieser, T., Bruton, C. J., Kieser, H. M., Lydiate, D. J., Smith, C. P., Ward, J. M., and Schrempf, H. (1985). Preparation of chromosomal, plasmid and phage DNA. In Genetic manipulation of streptomycetes: a laboratory manual, (Norwich, UK; John Innes Foundation), pp. 69-74.

Hui, J. P. M., Yang, J., Thorson, J. S., and Soo, E. C. 2007. Selective detection of sugar phosphates by capillary electrophoresis/mass spectrometry and its application to an engineered *E. coli* host. Chembiochem 8, 1180-1188.

Krauth, C., Fedoryshyn, M., Schleberger, C., Luzhetskyy, A., and Bechthold, A. (2009). Engineering a function into a glycosyltransferase. Chem. Biol. 16, 28 – 35.

Komaki, H., Izumikawa, M., Ueda, J.-Y., Nakashima, T., Khan, S. T., Takagi, M., and Shin-ya, K. (2009). Discovery of a pimaricin analog JBIR-13, from *Streptomyces bicolor* NBRC 12746 as predicted by sequence analysis of type I polyketide synthase gene. Appl. Microbiol. Biotechnol. 83, 127 - 133.

Liang, D., and Qiao, J. (2007). Phylogenetic analysis of antibiotic glycosyltransferases. J. Mol. Evol. 64, 342-353.

McNamara, C. M., Box, S., Crawforth, J. M., Hickman, B. S., Norwood, T. J., and Rawlings, B. J. (1998), Biosynthesis of amphotericin B. J. Chem. Soc. Perkin Trans. 1, 83-87.

Melançon, C. E., Hong, L., White, J. A., Liu, Y., and Liu, H.-W. (2006). Characterisation of dTDP-4-keto-6-deoxy-D-glucose 3, 4 ketoisomerase from the D-mycaminose biosynthetic pathway of *Streptomyces fradiae*: *in vitro* activity and substrate specificity studies. Biochemistry 46 (2), 577-590.

Mendez, C., and Salas, J. A. (2007). Engineering the glycosylation of natural products in actinomycetes. Trends Microbiol. 15, 219 – 232.

Naundorf, A., and Klaffke, W. (1996). Substrate specificity of native dTDP-D-glucose 4, 6-dehydratase: chemoenzymatic syntheses of artificial and naturally occurring deoxysugars. Carbohydrate Research 285, 141-150.

Nedal, A., Sletta, H., Brautaset, T., Borgos, S. E. F., Sekurova, O. N., Ellingsen, T. E. and Zotchev, S. B. (2007). Analysis of the mycosamine biosynthesis and attachment genes in the nystatin biosynthetic gene cluster of *Streptomyces noursei* ATCC 11455 Appl. Envir. Microbiol. 73, 7400 - 7407.

Nic Lochlainn, L., and Caffrey, P. (2009). Phosphomannose isomerase and phosphomannomutase gene disruptions in *Streptomyces nodosus*: impact on amphotericin biosynthesis and implications for glycosylation engineering. Metabolic engineering 11, 40-47.

Park, S. –H., Park, H.-Y., Sohng, J. K., Lee, H. C., Liou, K., Yoon, Y. J., and Kim, B.-G. (2009). Expanding substrate specificity of GT-B fold glycosyltransferase via domain swapping and high throughout screening. Biotechnology and Bioengineering 102 (4), 988-994.

Pawlak, J., Sowinski, P., Borowski, E., and Gariboldi, P. (1995). Stereostructure of perimycin A. Journal of Antibiotics 48, 1034-1038

Pfoestl, A., Hofinger, A., Kosma, P., and Messner, P. (2003). Biosynthesis of dTDP-3-acetamido-3, 6-dideoxy-α-D-galactose in *Aneurinibacillus thermoaerophilus* L420-91^{T}. J. Biol. Chem. 278, 26410 - 26417.

Power, P., Dunne, T., Murphy, B., Nic Lochlainn, L., Rai, D., Borissow, C., Rawlings, B., and Caffrey, P. (2008). Engineered synthesis of 7-oxo and 15-deoxy-15-oxo amphotericins: insights into structure-activity relationships in polyene antibiotics. Chem. Biol. 15, 78-86.

Schell, U., Haydock, S. F., Kaja, A. L., Carletti, I., Lill, R. E., Read, E., Sheehan, L., Low, L., Fernandez, M.-J., Grolle, F., McArthur, H. A. I., Sheridan, R., Leadlay, P. F., Wilkinson, B., and Gaisser, S. (2008). Engineered biosynthesis of hybrid macrolide polyketides containing D-angolosamine and D-mycaminose moieties. Org. Biomol. Chem. 6, 3315 - 3327.

Soler, L., Caffrey, P., and McMahon, H. E. M. (2008). Effects of new amphotericin analogues on the scrapie isoform of the prion protein. Biochim. Biophys. Acta 1780, 1162-1167.

Sullivan, F. X., Kumar, R., Kriz, R., Stahl, M., Xu, G.-Y., Rouse, J., Chang, X.-J., Boodhoo, A., Potvin, B., and Cumming, D. A. (1998). Molecular cloning of human GDP-mannose 4, 6 dehydratase and reconstitution of GDP-fucose biosynthesis *in vitro*. J. Biol. Chem. 273, 8193-8202.

Tello, M., Rejzek, M., Wilkinson, B., Lawson, D. M., and Field, R. A. (2008). Tyl1a, a TDP-6-deoxy-D-xylo-4-hexulose 3, 4-isomerase from *Streptomyces fradiae*: structure

prediction, mutagenesis and solvent isotope incorporation experiments to investigate reaction mechanism. Chembiochem 9, 1295-1302.

te Welscher, Y. M., ten Napel, Y. M., Balagué, M. M., Souza, C. M., Riezman, H., de Kruijff, B., and Breukink, E. (2008). Natamycin blocks fungal growth by binding specifically to ergosterol without permeabilizing the membrane. J. Biol. Chem. 283, 6393 - 6401.

Truman, A., Dias, M. V. B., Wu, S., Blundell, T. L., Huang, F., and Spencer, J. B. (2009). Chimeric glycosyltransferases for the generation of hybrid glycosyltransferases. Chem. Biol. 16, 676 - 685.

Thibodeaux, C., Melancon, C. E., and Liu, H.-W. (2007). Unusual sugar biosynthesis and natural product glycodiversification. Nature 446, 1008-1016

Weymouth-Wilson, A. C. (1997). The role of carbohydrates in biologically active natural products. Nat. Prod. Reports 14, 99 – 110.

Williams, G. J., Zhang, C., and Thorson, J. S. (2007). Expanding the promiscuity of a natural product glycosyltransferase by directed evolution. Nature Chemical Biology 3, 657 – 662.

Williams, G. J., Goff, R. D., Zhang, C., and Thorson, J. S. (2008a). Optimising glycosyltransferase specificity via "hot-spot" saturation mutagenesis presents a catalyst for novobiocin glycorandomisation. Chem. Biol. 15, 393 – 401.

Williams, G. J., Gantt, R. W., and Thorson, J. S. (2008b) The impact of enzyme engineering upon natural product glycodiversification. Curr. Op. Chem. Biol. 12, 556 - 564.

Zhang, C., Moretti, R., Jiang, J., and Thorson, J. S. (2008). The *in vitro* characterisation of polyene glycosyltransferases AmphDI and NysDI. Chembiochem 9, 2506-2514.

Zhao, L., Ahlert, J., Xue, Y., Thorson, J., Sherman, D., and Liu, H.-W. (1999). Engineering a methymycin/pikromycin-calicheamicin hybrid: construction of two new macrolides carrying a designed sugar moiety. J. Am. Chem. Soc. 121, 9881-9882

Zhao, G., Liu, J., Liu, X., Chen, M., Zhang, H., and Wang, P. G. (2007). Cloning and characterization of GDP-perosamine synthetase (Per) from *Escherichia coli* O157:H7 and synthesis of GDP-perosamine *in vitro*. Biochem. Biophys. Res. Commun. 363, 525-30.

Table 1. Oligonucleotides used in this study

Oligonucleotide	Sequence 5′ to 3′
PerDIIIF	AAAAGGATCCTGAAAGGGGACCATATGCCAAGCGCGCGCTGATC
PerDIIIR	AAAAAAGCTTCCCTAGTGATGCCGCGGGCTAC
BM1	TTCCAAGCTTCATCACAGGACTCCGTAGAAGGC
BM2	GAAGTCACATATGTCCTATACGTATCCGGTC
PerDIIR	GATCAAGCTTCAGCCCCCGTGCGCTGCGACCGC
PerDIIF	GACCAGATCTTCGGCCTGCCGAGCCTGTCCT
AmphDIIF	TGACAGATCTGACCGAGGAAGTCAAGGATG
AmphDIIR	GATCAAGCTTCATCTCGGTCTCGGCGGTCATCA
GTF1	CAACGAGCTCTTCAAATTCCGCACGCTGGGC
GTF3	GGCGGAGCTCGAGTACCCGCTGGAGATCCCG
GTR3	AGTCGAGCTCCGCCACCGAGTAGCAC
GTR1	GGAAGAGCTCGTTCTCCACCCGCTGG
OGTF	GCATAGATCTCACTTTCCGGAGGGTGTTGTCCATG
OGTR	GATCAAGCTTCAGCCCCCGTGCGCTGCGACCGC

Figure legends

Figure 1. Structure of perimycin

Figure 2. Biosynthetic pathways to GDP-perosamine and GDP-mycosamine in *S. aminophilus* and *S. nodosus*.

Figure 3. Amphotericins discussed in this work: **2**, amphotericin B; **3**, amphotericin A; **4**, 8-deoxy-16-descarboxyl-16-methyl-amphoteronolide B; **5**, 8-deoxy-16-descarboxyl-16-methyl-amphoteronolide A; **6**, 8-deoxyamphoteronolide B; **7**, 8-deoxyamphoteronolide A; **8**, 16-descarboxyl-16-methyl-19-O-deoxymannosyl-amphoteronolide B; **9**, 8-deoxy-16-descarboxyl-16-methyl-19-O-deoxymannosyl-amphoteronolide A; **10**, 19-O-deoxymannosyl-amphoteronolide B; **11**, 19-O-perosaminyl-amphoteronolide B; **12**, 16-descarboxyl-16-methyl-19-O-perosaminyl-amphoteronolide B.

Figure 4. Inactivation of *amphDII*. A. Replacement of *amphDII* with a mutant version results in loss of a chromosomal NcoI site (N). An adjacent BclI site (B) is unaffected. The small arrows represent the BM1 and BM2 primers used to amplify the *amphDII* region from chromosomal DNA. B. Analysis of *amphDII* region in various strains. The *amphDII* region was amplified by PCR and treated with restriction enzymes. The wild type *amphDII* region contained the expected NcoI site (lane 1) whereas the corresponding

sequences from the *amphDII* (lane 2) and *amphDII-NM* (lane 3) mutants did not. All three PCR products were digested by BclI in control digests (lanes 4 to 6).

Figure 5. Detection of perosaminylated polyene by HPLC. Panel A shows HPLC analysis of polyenes produced by *S. nodosus* Δ*amphDII* transformed with pIAGO. Panel B shows polyenes extracted from the same host carrying pIAGO-*perDII*. Panel C shows polyenes from the strain carrying pIAGO-*hap2* encoding the Hap2 hybrid GT and PerDII.

Figure 1

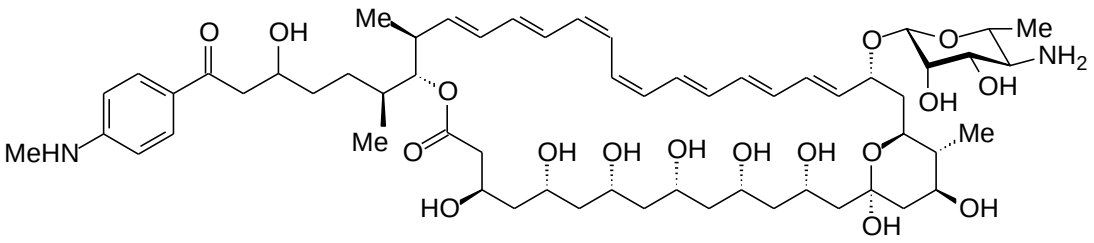

Perimycin
1

Figure 2

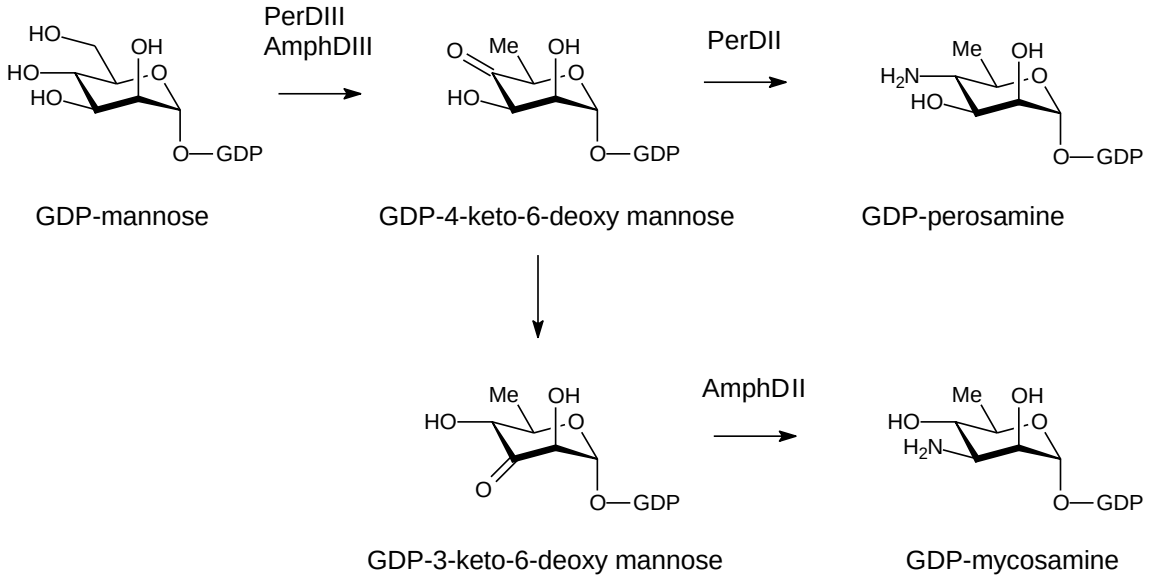

Figure 3

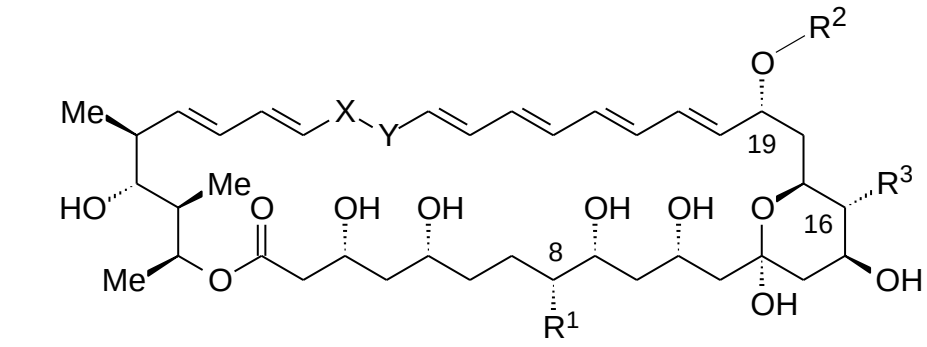

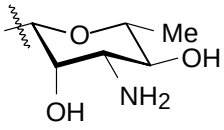

Mycosamine

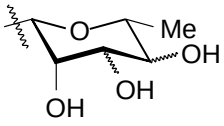

6-Deoxyhexose

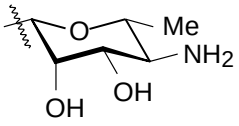

Perosamine

Compound	R^1	R^2	R^3	X-Y	RMM
2	OH	Mycosamine	COOH	HC=CH	923.5
3	OH	Mycosamine	COOH	H_2C-CH_2	925.5
4	H	H	CH_3	HC=CH	732.5
5	H	H	CH_3	H_2C-CH_2	734.5
6	H	H	COOH	HC=CH	762.5
7	H	H	COOH	H_2C-CH_2	764.5
8	OH	6-Deoxyhexose	CH_3	HC=CH	894.5
9	H	6-Deoxyhexose	CH_3	H_2C-CH_2	880.5
10	OH	6-Deoxyhexose	COOH	HC=CH	924.5
11	OH	Perosamine	COOH	HC=CH	923.5
12	OH	Perosamine	CH_3	HC=CH	893.5

Figure 4

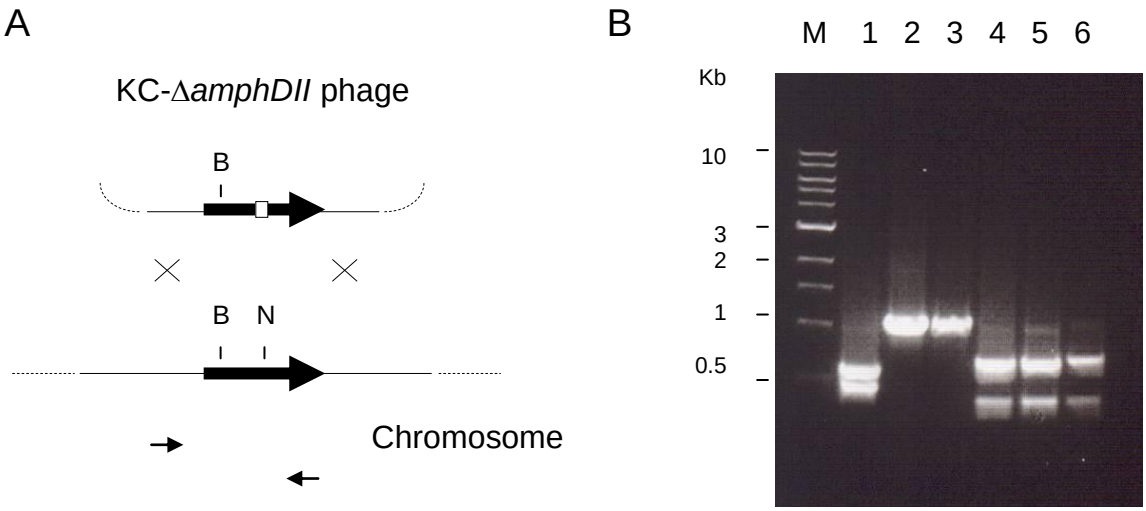

Figure 5

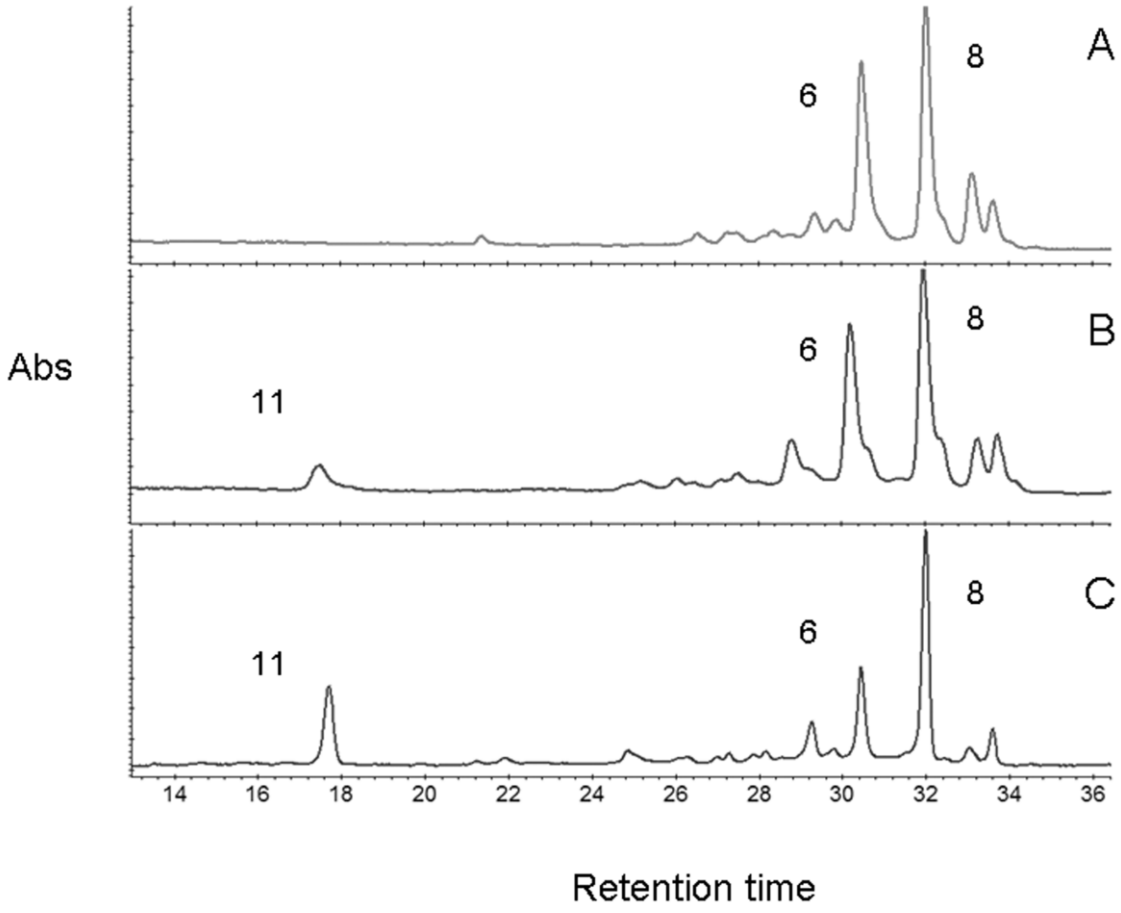

Supplemental information

Redesign of polyene macrolide glycosylation: engineered biosynthesis of perosaminyl-amphoteronolide B

Running title: Redesign of amphotericin glycosylation

Eve Hutchinson[1], Barry Murphy[2], Terence Dunne[1], Ciaran Breen[1], Bernard Rawlings[2] and Patrick Caffrey[1]*

[1]School of Biomolecular and Biomedical Science and Centre for Synthesis and Chemical Biology, University College Dublin, Belfield, Dublin 4, Ireland.

[2]Department of Chemistry, University of Leicester, University Road, Leicester LE1 7RH, United Kingdom

*Corresponding author. E-mail: patrick.caffrey@ucd.ie

Complete NMR data is available from Dr. Bernard Rawlings, bjr2@leicester.ac.uk

Inventory of supplemental information

Gene	Gene product	Function
amphDIII	AmphDIII, GDP-mannose 4,6 dehydratase	Catalyses conversion of GDP-mannose to GDP-4-keto-6-deoxymannose
amphDII	AmphDII, GDP-mycosamine synthase	Catalyses transamination of GDP-3-keto-6-deoxymannose to GDP-mycosamine
amphDI	AmphDI, mycosaminyltransferase	GT that transfers mycosaminyl residue from GDP to 8-deoxyamphoteronolides A and B
amphN	AmphN, cytochrome P450	Formation of exocyclic carboxyl group of amphotericin B. Catalyses conversion of 8-deoxy-16-descarboxyl-16-methyl-amphoteronolides A and B to 8-deoxyamphoteronolides A and B
amphL	AmphL, cytochrome P450	Catalyses C-8 hydroxylation of 8-deoxyamphoteronolides A and B.
perDIII	PerDIII, GDP-mannose 4,6 dehydratase	Catalyses conversion of GDP-mannose to GDP-4-keto-6-deoxymannose
perDII	PerDII, GDP-perosamine synthase	Catalyses transamination of GDP-4-keto-6-deoxymannose to GDP-perosamine
perDI	PerDI, Perosaminyltransferase	GT that transfers perosaminyl residue from GDP to perimycin aglycone
hap1	Hap1, hybrid AmphDI-PerDI GT 1	Residues 1 to 191 of AmphDI fused to residues 192 to 458 of PerDI. Non-functional.
hap2	Hap2, hybrid AmphDI-PerDI GT 2	Residues 1 to 246 of AmphDI fused to residues 245 to 458 of PerDI. Catalyses transfer of perosaminyl residue from GDP to perimycin aglycone

Table S1. (Related to Figure 2) Genes involved in modification of amphotericin and perimycin aglycones.

Figure S1

A
Glycosyltransferases

```
PerDI          MDPARRPILFASLPESGLLNPLLVLAGELSRQGVEDLWFATDEPGAEDVRRVATGAPVEF 60
AmphDI         MGAHRRPILFVSYAESGLLNPLLVLAEELSRRGVEDLWFATDEKARDQIESASADSELQF 60
NysDI          MGANRRPILFVSYAESGLLNPLLVLAGELSRRDVADLWFATDEKARDEVAAVVDGSPVRF 60
PimK           MESARRPILFVSLPESGLLNPLLVLAGELSRQGVEDLWFATDEPRRNDVKRIAEGSPVEF 60
RimE           MESARRPILFVSLPEAGLANPLLVLAEELSRQGVEDLWFATDEPRREDVKKISVGSPVEF 60
CanG           MDSAARPILFVSLPESGLLNPLLVLAGELARRGVPDLWFATDEHRREEVEALSDVSKVSF 60
FscM1          MDSAARPILFVSLPESGLLNPLLVLAGELARRGVPDLWFATDEHRREEVEALSDVSKVSF 60

PerDI          ASLGEVAPELSAGTWPEDVYREVTHSSRFRAHRAIIKQSYRPAIQAEKFRRLEEIVEKVR 120
AmphDI         ASLGDTVSQMSAVTWDDETYAEVTQRSRFKAHRAVIRHSFAPETRVEKYRALEKAVEEIQ 120
NysDI          ASLGDTVSQMSAVTWDDATYAEVTQRSRFKAHAAVIRHSFAPESRMAKYRRLEEIVEEVE 120
PimK           ASLGEVDSEMSAVTWSDEVYREVTQPSRFKAHRAVVRHTYRPGLQAEKFRRLQAVIDEVQ 120
RimE           ASLGEVVPELSAVTWGDEVYREVTQPSRFKAHRAVIRHSYVPRAQEEKFQKLAAVVDEIR 120
CanG           ASLGEVVPELSAVTWDDEVYREVTQSSRFKAHRAVVRQSYRPALQARKYRELEQVVDEVR 120
FscM1          ASLGEVVPELSAVTWDDEVYREVTQSSRFKAHRAVVRQSYRPALQARKYRELEQVVDEVR 120

PerDI          PALMVVDCTSGFAVDLAVAREIPFVLSVPYLPSNVLVPHHPFAKGYAPRNFPVPHSGLPH 180
AmphDI         PALMVIESMCQFGYELAITKGIPFVLGVPFLPSNVLTSHVPFAKSYTPSGFPVPHSGLPG 180
NysDI          PALMVIESMCQFGYELAITKGIPFVLGVPFVPSNVLTSHVPFAKSYTPSGFPVPHSGLPA 180
PimK           PALMVIDCISGFAVDAAIARNIPYVLSVPFLPSNVLTAHTHFAKSYTPRGFPVPHTGLSR 180
RimE           PALIVVDCISSYGVELAMARKIPYVLSVPFLPSNVLTAFTPFAKGYTPKDFPVPHTGLPY 180
CanG           PALMVVDCVAGFGVDLALARGIPYVLNVPFVASNVLTSHNPFGASYTPKSFPVPNSGLPA 180
FscM1          PALMVVDCVAGFGVDLALARGIPYVLNVPFVASNVLTSHNPFGASYTPKSFPVPNSGLPA 180

                        ** Hap1
PerDI          PMTPAQRLANELFKFRTLGMFLTPSMGKVLAEDSRIRKELKLPPPT--PMTRIEKAELVL 238
AmphDI         KMSLAQRVENELFRVRTLGMFMTKEIREIVEEDNRVRGELGISPEARQMMARIDHAEQVL 240
NysDI          AMSLAQRIENQLFRLRTLGMFLTSDVRKVVEEDNRVRTELGIAPQARQMMARIDHAEQVL 240
PimK           RMTLAQRVANELFKLRTFAMFLNPRLGKVLAEDNRRRNELGLPKAS--FMARIEHADLVL 238
RimE           PMNLPQRVRNMLFKLRTFAMFCNPTMSKVLAEDNRRRKAHGLGQMS--PMARIDHADLVL 238
CanG           RMSVRQKLANTLFKWRTLGMFLHPDMAALLREDAAIRKELGIAPPN--AMTRVDEAAAVV 238
FscM1          RMSVRQKLANTLFKWRTLGMFLHPDMAALLREDAAIRKELGIAPPN--AMTRVDEAAAVV 238

                     ** Hap2
PerDI          CTSVAELEYPLEIPEKMRLVGALLPPLPQTSGDDPVRAWLDAQSSVVYMGFGTVTRLTGQ 298
AmphDI         CYSVAELDYPFPMHEKVRLVGTLVPPLPQAPDDEGLSDWLTEQKSVVFMGFGTITRLTRE 300
NysDI          CYSVRELDYPFPMHPKLRLVGTMVPPLPQAPDDDGLSDWLSAQKSVVYMGFGTITRLTRE 300
PimK           CNSLAELDYPFDIPEKMRLVGAMVPPLPEAPDDQDLSRWLDAQSSVVYVGLGTITRLTRE 298
RimE           CNSIAELDYPFDIPEKFRMVGTMVPPLPEAEQEDELSRWLDEQPSVVYAGFGTITRLTRE 298
CanG           CSSVAELDYPFDIPDRVSLVGAVLPPLPEAPDDDEVTRWLDAQSSVVYMGFGTITRLTRE 298
FscM1          CSSVAELDYPFDIPDRVSLVGAVLPPLPEAPDDDEVTRWLDAQSSVVYMGFGTITRLTRE 298

PerDI          QVHALVEVARRLDGE-HQVLWKLPAEQQHLLPPAESLPGNLRIESWVPSQLDVLAHPHVR 357
AmphDI         QVASLVEVARRLEGEGHQVLWKLPSEQQHLLPPAEELPANLRIESWVPSQLDVLAHPNVK 360
NysDI          QVASLVEVARRLDGRGHQVLWKLPRGQQELLPPAAELPDNLRIEGWVPSQLDVLAHPNVK 360
PimK           QVGSMVEVARRLEDR-HQVLWKLPSEQQHLLPPRESLPGNLRVESWVPSQMDVLAHPHVK 357
RimE           QVHSMVEVARRLQGR-HQVLWKLPSGQQHLLPPKESLPDNLRIENWVPSQLDVLAHPNVK 357
CanG           EVAALVEVARRMSGT-HQFLWKLPKEQQHLLPEAGSLPDNLRVESWVPSQLDVLAHPNVS 357
FscM1          EVAALVEVARRMSGT-HQFLWKLPKEQQHLLPEAGSLPDNLRVESWVPSQLDVLAHPNVS 357
```

```
PerDI          VFFTHGGGNGFHEGLYFDKPLVVRPLWVDCYDQAVRGRDRGVSLTLDDPGDIVVDDVVDK 417
AmphDI         VFFTHAGGNGYHEGLYFGKPLVVRPLWVDCDDQAVRGQDFGVSLTVDRPETVDTDDVLDK 420
NysDI          AFFTHAGGNGYHEGLYFGKPLVVRPLWVDCDDQAIRGQDFGVSLTLDRPETVDTEDVLDK 420
PimK           VFFTHGGGNGFNEGMYFGKPLVVRPLWVDCYDQAVRGQDFGLSLTLDRPQTIDVNDVVDK 417
RimE           LFFTHAGGNGYNEGVYFGKPQVVRPLWVDCYDQAVRGRDFGISLTLDRPRDLDVDDVVDK 417
CanG           VFFSHGGGNAYHEGVYFGKPQVVRPLWVDCFDQAVRGRDFGISLTLDKPHTVDPDDVVDK 417
FscM1          VFFSHGGGNAYHEGVYFGKPQVVRPLWVDCFDQAVRGRDFGISLTLDKPHTVDPDDVVDK 417

PerDI          LTRVLTEPSFRANAARMGALQRAAGGRAAAADLILGLPSLS                     458
AmphDI         ITRVLNESSFTERAEYYAGLLKAAGGRTAAADLLLGLPVLA                     461
NysDI          ITRVLDQPSFTERAEHFAGLLRDAGGRAAAADLLLGLPALA                     479
PimK           LTRVLGTPSFYEKAERRAALMRSAGGRETAAGLVLSLPALA                     458
RimE           LTRVLETPSFRENAERLGALQRAAGGRAAAAEVILGHPALARA                   460
CanG           LTRVTSDPAFRTEAERLGALQRAAGGRAAAADLVTGLLPAA                     458
FscM1          LTRVTSDPAFRTEAERLGALQRAAGGRAAAADLVTGLLPAA                     458
```

B
Perosamine and mycosamine synthases

```
PerDII           MSFKYPASRPALDGRELEYVTETIRDGWISSQSPVVQRFEEAFAAYHGTVHGVACSSGTA 60
AmphDII          MSYTYPVSMPWLKGRELEYVTEAVSGGWISSQGPYVRQFEEAFAAYNDMPHGVACSSGTT 60
NysDII           MSFTYPVSMPWLQGRELDYVTEAVGGGWISSQGPYVRRFEEAFAAYNDVPFGVACSSGTT 60
PimC             MSFKYPVSRPTLDGRELEYVTGAVGDGWISSQGPMVARFERAFADYNGVAHGVSCSSGTA 60
RimF             MSFKYPVSRPALEGNELAYLTGAVEDGWISSQGPMVGRFERAFADYNGIAHGVSCSSGTA 60
CanA             MAFTHPVSRPALDGRELEYVSDAVSGGWISSQGPYVRRFEEAFAEWNGVAHGVACSSGTA 60
FscMII           MAFTHPVSRPALDGRELEYVSDAVSGGWISSQGPYVRRFEEAFAEWNGVAHGVACSSGTA 60

PerDII           ALTLALRALGIGPGDEVIVPEFTFITSAWAVTYTGATPVFVDCGDDLDIDVELIEKKITP 120
AmphDII          ALTLALRALGVGPGDEVIVPEFTMIATAWAVTYTGATPVFVDCGDDLNIDVSRIEEKITP 120
NysDII           ALTLALRALGVGPGDEVIVPEFTMIASAWAVTYTGATPVFVDCGDDLNIDVSRIEEKITP 120
PimC             ALTLALRALGIGPGDEVIVPEFTMVASAWAVTYTGATPVFVDCGDDLNIDVTRIEEKITA 120
RimF             ALTLALRALGIGPGDEVIVPEFTMIASAWAVTYTGATPVFVDCGDDLNIDVTRIEEKITA 120
CanA             ALTLALRALNIGPGDEVIVPEFTMVASAWAVTYTGATPVFVDCGDDLNIDVTRIEEKITP 120
FscMII           ALTLALRALNIGPGDEVIVPEFTMVASAWAVTYTGATPVFVDCGDDLNIDVTRIEEKITP 120

PerDII           RTKAVMPVHVYGRRCDMATIMELAFEYNLRVVEDSAEAHGVRPVGDIACFSLFANKTVTA 180
AmphDII          RTKVIMPVHIYGRQCDMDAIMNLAYEYNLRVVEDSAEAHGVRPVGDIACFSLFANKIITA 180
NysDII           RTKVIMPVHIYGRQCDMDAVLNLAYEYNLRVVEDSAEAHGVRPRGDIACFSLFANKIISA 180
PimC             RTKAVMPVHIYGRRCDMDAVMDIAHQYNLRVVEDSAEAHGVRPVGDIACYSLFANKIITA 180
RimF             RTKAVMPVHIYGRRCDMDAIMDIAYQYNLRVVEDSAEAHGIRPVGDIACYSLFANKIITA 180
CanA             RTRAVMPVHVYGRRCDMDAVMDLALQYNLRVVEDSAEAHGVRPVGDIACFSLFANKIITA 180
FscMII           RTRAVMPVHVYGRRCDMDAVMDLALQYNLRVVEDSAEAHGVRPVGDIACFSLFANKIITA 180

PerDII           GEGGVCLTDDPRLARQMAHLRAMATPADHSYLHKNLAYNFRMTGMQAAVALAQVERMDEI 240
AmphDII          GEGGVCVTRDAHLAEQMAHLRAMAFTKDHSFLHKKLAYNYRMTNMQAAVALAQTEQLDTI 240
NysDII           GEGGVCLTHDPHLAEQMAHLRAMAFTKDHSFLHKKLAYNFRMTNMQAAVALAQTEQLDTI 240
PimC             GEGGICLTDDPRLAGQLAHLRAMAFTKDHSFLHKKVAYNFRMTAMQAAVALAQVERLDDI 240
RimF             GEGGICLTDDPKLAGQMQHLRAMAFTKDHSFLHKKVAYNYRMTAMQAAVALAQTERLDDI 240
CanA             GEGGVCLTDDPRLAEQLAHLRAMAFTRDHSFLHKKLAYNYRMTAMQGAVALAQTERLDEI 240
FscMII           GEGGVCLTDDPRLAEQLAHLRAMAFTRDHSFLHKKLAYNYRMTAMQGAVALAQTERLDEI 240

PerDII           LATRRTIEKRYDTLLAGIPGLTLMPPRDVLWMYDVRAQQREELRAFLAEASIETRLFFKP 300
AmphDII          LATRRDIEKRYDEALRDVPGITLMPARDVLWMYDLRAERSEELRAYLADQGVETRVFFKP 300
NysDII           LALRRDIEKRYDEALRDIPGITLMPPRDVLWMYDLRAERRDELCAYLAGEGIETRVFFKP 300
PimC             LATRREIERRYDEGLAGVPGITLMPPRDVLWMYDLRAERREELREFLAGESIETRLFFKP 300
RimF             LEVRRGIEKRYDEGLADVPGITLMPPRDVLWMYDLRAERREELREFLAGESIETRLFFKP 300
CanA             LATRREIEARYDAGLKDLPGITLMPARDVLWMYDLRAERREELRAHLDERGIETRLFFKP 300
FscMII           LATRREIEARYDAGLKDLPGITLMPARDVLWMYDLRAERREELRAHLDERGIETRLFFKP 300
```

```
PerDII          MSRQPTYFHPDWRSLNAGRFSEDGLHLPTYTALTEEDQAYVAGKIREFYARAPSGRAVAA 360
AmphDII         MSRQPGYYDANWPSLNASRFSEDGFYLPTHTGLTAQDQEFITDRVRAFYGVL-------- 352
NysDII          MSRQPGYFSADWPALNAARLSADGFYLPTHTGLTAQEQEFITGRIRAFYGVA-------- 352
PimC            MSRQPMYFHPDWPSLKAHTFAEDGLYLPTHTGLSATDQDFVIDRVRAFYGAS-------- 352
RimF            MSRQPMYFHPDWPSLKANTFAEDGLYLPTHTGLTAGDQDFVIDRVRAFYGVG-------- 352
CanA            MSRQPGYLDPVWPTLNAHRFSEDGLYLPTHTGLTAADQEYITGAVRDFYRAG-------- 352
FscMII          MSRQPGYLDPVWPTLNAHRFSEDGLYLPTHTGLTAADQEYITGAVRDFYRAG-------- 352

PerDII          HGG 363
```

C
GDP-mannose 4,6 dehydratases

```
PerDIII         MSKRALITGITGQDGSYLAEHLLQQGYQVWGLTRGQANPRKDRVSRLIPELQFVSGDMMD 60
AmphDIII        MPKRALITGITGQDGSYLAEHLLSQGYQVWGLIRGQANPRKFRVSRLASELSFVDGDLMD 60
NysDIII         MSKRALITGITGQDGSYLAEHLLSQGYQVWGLIRGQANPRKSRVSRLASELDFIDGDLMD 60
PimJ            MSKRALITGITGQDGSYLAEHLLAQGYQVWGLIRGQANPRKSRVSRLVSELSFVDGDLMD 60
FscMIII         MSKRALITGITGQDGSYLAEHLLDQGYQVWGLCRGQANPRKDRIAKLIPELSFVDGDLMD 60

PerDIII         QGSLVAAVDVVQPDEIYNLGAISFVPMSWQQAELVTEVNGTGVLRMLEAVRMVSGFGRSA 120
AmphDIII        QGSLVSAVDKVQPDEVYNLGAISFVPMSWQQAELVTEVNGMGVLRVLEAIRMVSGLSMSR 120
NysDIII         QGSLVSAVDTVQPDEVYNLGAISFVPMSWQQAELVTEVNGMGVLRMLEAIRMVSGLSTSR 120
PimJ            QSSLCSAVDKVQPDEIYNLGAISFVPMSWQQPELVTEINGMGVLRMLEAIRMVSGLNGSR 120
FscMIII         QGSLVSAVDLVQPDEVYNLGAISFVPMSWQQPELVTEVNGTGVLRMLEAVRIVSGLTKSS 120

PerDIII         GRDPSGQIRFYQASSSEMFGQVVESPQSELTSFHPRSPYGVAKAYGHYITQNYRESFGMY 180
AmphDIII        TAGTEGQIRFYQASSSEMFGKVAETPQRETTLFHPRSPYGAAKAYGHFITRNYRESFGMY 180
NysDIII         TVSPRGQIRFYQASSSEMFGKAAETPQRETTLFHPRSPYGAAKAYGHYITRNYRESFGMY 180
PimJ            SDG-GGQIRFYQASSSEMFGKVAETPQRETTIFRPRSPYGVAKTYGHFITRNYRESFGMY 179
FscMIII         GGSPRGQIRFYQASSSEMYGKVAESPQRETTSFHPRSPYGVAKAFGHYITQNYRESYGMY 180

PerDIII         GVSGILFNHESPRRGAEFVTRKISLAVAQIKLGLQDKLALGNLDAVRDWGFAGDYVRAMH 240
AmphDIII        AVSGMLFNHESPRRGQEFVTRKISLAVARIKLGLQDKLALGNMDAVRDWGYAGDYVRAMH 240
NysDIII         AVSGMLFNHESPRRGQEFVTRKISLAVARIKQGLQDKLALGNLDAVRDWGYAGDYVRAMH 240
PimJ            AVSGMLFNHESPRRGAEFVTRKISLAVARIKLGYQDKLSLGNLDAVRDWGFAGDYVRAMH 239
FscMIII         GVSGILFNHESPRRGAEFVTRKISLAVAQIKLGQMDKLHLGNLDAERDWGFAGDYVRAMH 240

PerDIII         LMLSQDSPADYVIGTGRMHSVREAARIAFECVGLDWEQHVVVDPALVRPAEVETLCADCG 300
AmphDIII        LMLQQDAPDDYVIGTGEMHTVRDAVRFAFEHVGLDWKDYVVVDPDLVRPAEVEVLCADSS 300
NysDIII         LMLQQDAGDDYVIGTGQMHSVRDAVRIAFEHVGLNWEDYVVIDPDLVRPAEVEVLCADSA 300
PimJ            LMLQQDEPGDYVIGTGEMHSVRDAVRIAFEHVGLNWEDYVSIDPSLVRPAEVEILCADAE 299
FscMIII         LMLQQEQAGDYVVGTGAMHQVRDAARIAFEHVGLDWQEHVVVDPGLVRPAEVETLCADSG 300

PerDIII         KAREVLGWEQTVEFPELIQMMVESDLRMAGQTRDHGKLLTAASW 344
AmphDIII        KAQAQLGWKPSVDFQELMRMMVDADLASVSRQNELDDLLLAHSW 344
NysDIII         KAQDRLGWKPDVDFPTLMRMMVDSDLAQVSRENQYGDVLLAANW 344
PimJ            RARTQLGWEPSVDFPELMRMMVDSDLRQASREREYGDLLLAASW 343
FscMIII         NARRELGWEPEVDFEQLMRMMVESDLRQASRERDYSQLLATGSW 344
```

Figure S1. (Related to Figure 2). Sequence alignments of proteins involved in perosaminylation and mycosaminylation of polyene aglycones. A. Glycosyltransferases; B, Perosamine and mycosamine synthases; C, GDP-mannose 4, 6 dehydratases. Enzymes involved in mycosamine biosynthesis and attachment are from the producers of amphotericin B, nystatin, pimaricin, rimocidin and candicidin/FR008. With PerDI, PerDII and PerDIII, the amino acid residues highlighted in bold differ from all of their counterparts involved in mycosaminylation. In panel A, the cross-over points for hybrid glycosyltransferases 1 and 2 are marked with asterisks.

Figure S2

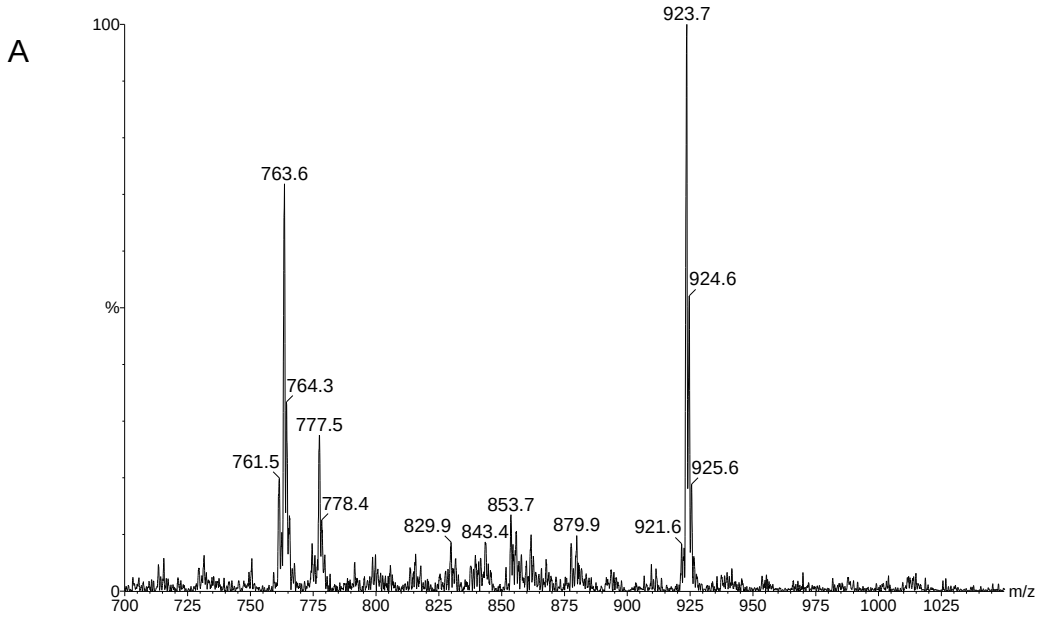

Figure S2. (Related to Figure 4). ESMS analysis of crude polyenes produced by *S. nodosus* Δ*amphDII* by ESMS in negative ion mode. The major ions correspond to 8-deoxyamphoteronolide B (**6**, $[M - H]^-$ = 761.5), 8-deoxyamphoteronolide A (**7**, $[M - H]^-$ = 763.5), amphoteronolide B ($[M - H]^-$ = 777.5) and 6-deoxyhexosyl-amphoteronolide B (**10**, $[M - H]^-$ = 923.5).

Figure S3

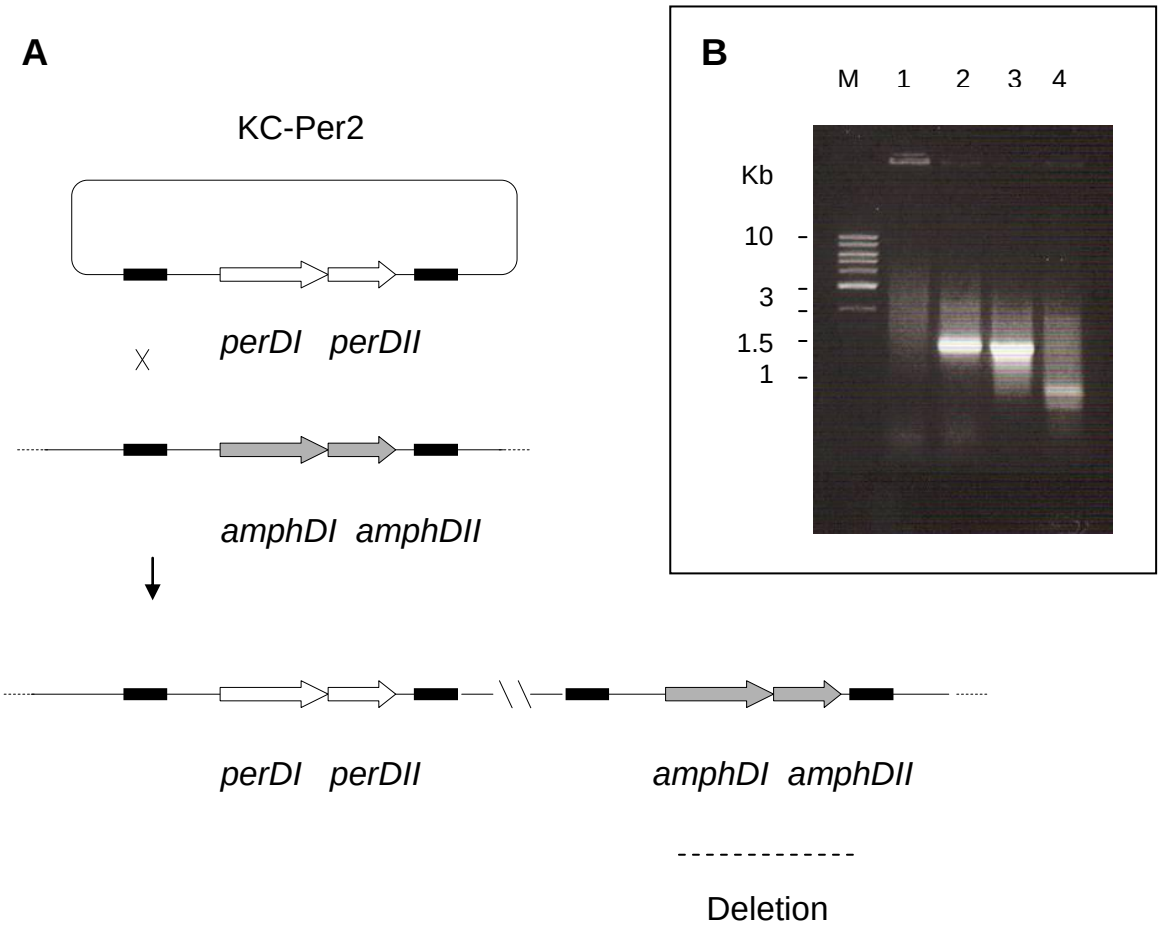
A
KC-Per2
perDI perDII
amphDI amphDII
perDI perDII
amphDI amphDII
Deletion
B
M 1 2 3 4
Kb
10
3
1.5
1

Figure S3. Formation of an *amphDI-DII-NM* mutant containing *perDI* and *perDII* genes. Phage KC-Per2 was designed to replace *amphDI-amphDII* with *perDI-DII* by a double cross-over recombination event in *S. nodosus* ΔNM. Plasmid subclone 382 contains a BamHI fragment corresponding to nucleotides 65288 to 69575 of the amphotericin biosynthetic gene cluster. This region contains most of the *amphA* gene and the 5′ end of *amphDI*. The start codon for the *amphDI* gene (Zhang et al., 2008) is located within an NcoI site (CCATGG). This sequence is conserved in the *perDI* gene where it surrounds the only plausible start codon. The *perDI-perDII* region was amplified with primers CBD1F and CBD2R (CBD1F = 5′ TTTTAGATCTGCCGGCCACCGATGAAAGG 3′ ; CBD2R = 5′ AAAACTGCAGGATCCTCAGCCCCCGTGCGCTGCGACC 3′). The 2.5 kb PCR product was digested with NcoI and PstI and ligated between the NcoI and PstI sites of plasmid p382 to form pAM-PER1. Ligation of the NcoI cohesive ends positions the *perDI* start codon at the optimal distance from the *amphDI* ribosome-binding site and promoter. A KpnI fragment containing excess upstream *amphA* DNA (nucleotides 65288 to 69575 of the cluster) was deleted to give pAM-PER2.

Oligonucleotides PC1 and PC2 were used to amplify a 960 bp stretch of DNA downstream from the *amphDI-DII-N-M* region [nucleotides 60151 – 61112] (PC1 = 5′ GATCAGATCTTGGTGGACGCTTCTTCCCCCGCTTTC 3′ ; PC2 = 5′ GATCAAGCTTGGATCCGTACGTCTGAAGTACATAAAAAACGGA 3′). This PCR product was digested with BglII and HindIII and cloned into BamHI-HindIII cut plasmid pAM-PER2 to form pAM-PER3. This plasmid contained the *perDI-DII* genes flanked by *amphDI-DII* upstream and downstream sequences. This sequence was excised with StuI and BamHI and cloned between the ScaI and BamHI sites of KC-UCD1 to give KC-Per2.

Panel A. Formation of the required genotype by a single cross-over and a fortuitous deletion. Panel B. Analysis of parent and mutant strains by PCR with primers specific for the *amphDI-DII* region and the *perDI-DII* region. The deletion mutant lacked *amphDI-DII* (lane 1) but not *perDI-DII* (lane 3). The parent strain *S. nodosus* ΔNM contained the *amphDI-DII* region (lane 2) but not the *perDI-DII* region (lane 4).

Figure S4

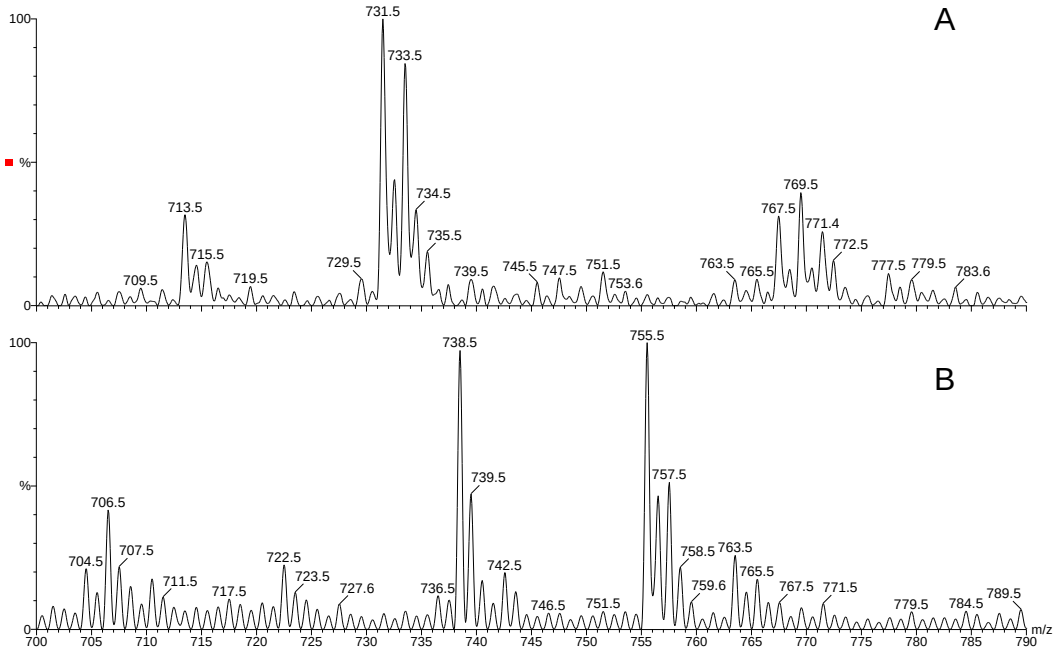

Figure S4. ESMS analysis of mixed tetraene and heptaene aglycones from *S. nodosus amphDI-DII-NM* mutant containing *perDI* and *perDII* genes. Panels A and B show analyses in negative and positive ion modes. A. The major ions correspond to 8-deoxy-16-descarboxyl-16-methyl-amphoteronolide B (**4**, $[M - H]^-$ = 731.5; $[M + Cl]^-$ = 767.5), 8-deoxy-16-descarboxyl-16-methyl-amphoteronolide B (**5**, $[M - H]^-$ = 733.5; $[M + Cl]^-$ = 769.5). B. These compounds were also detected in positive ion mode (**4**, $[M + Na]^+$ = 755.5; **5**, $[M + Na]^+$ = 757.5). The species with a mass of 738.5 in panel B is an unknown contaminant.

Figure S5

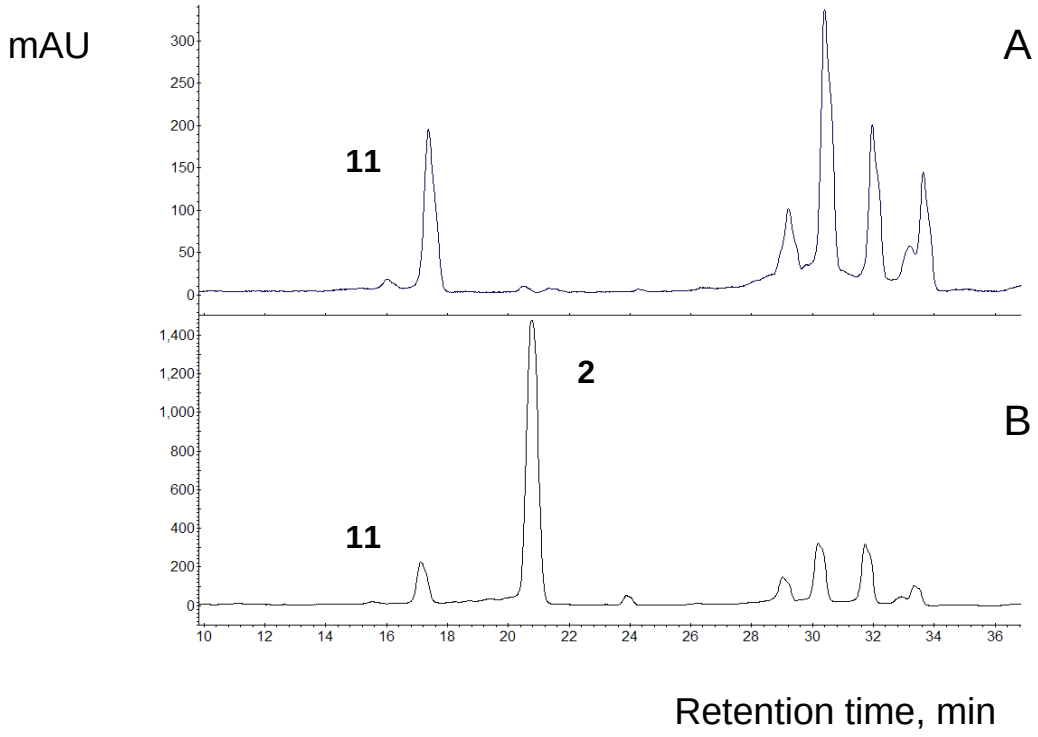

Figure S5. (Related to Figure 5). HPLC analysis of perosaminyl-amphoteronolide B (**11**) extracts spiked with amphotericin B (**2**). Chromatogram A shows analysis of an extract from *S. nodosus* Δ*amphDII* pIAGO-*hap2*. Chromatogram B shows the same extract spiked with amphotericin B.

Figure S6

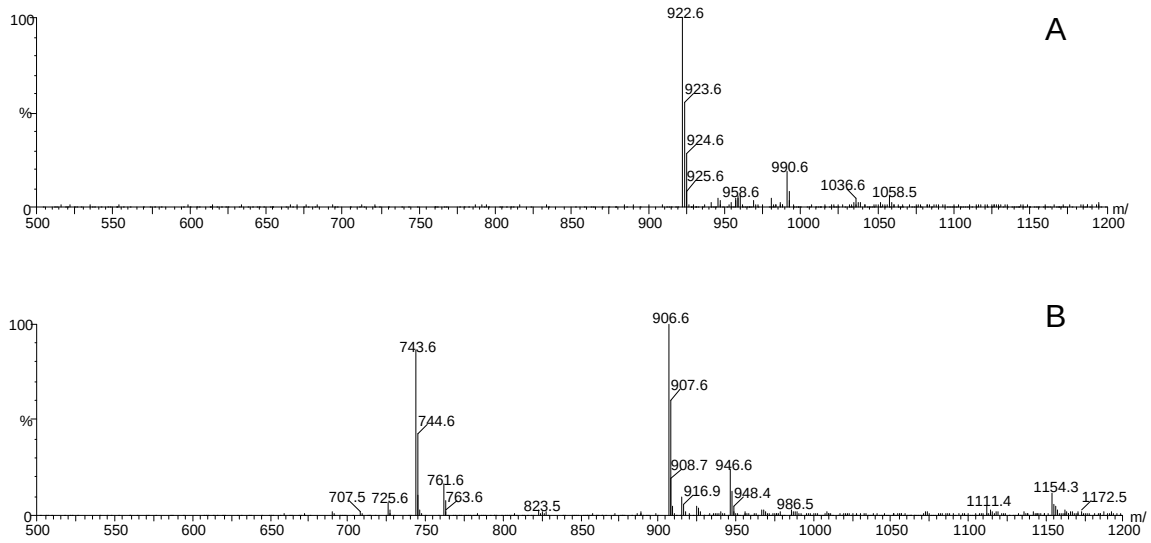

Figure S6. (Related to Figure 5). ESMS analysis of new heptaene purified from *S. nodosus* Δ*amphDII* pIAGO-*hap2*. A. Analysis in negative ion mode revealed the mass appropriate for **11** ($[M - H]^-$ = 922.5). B. Analysis in positive ion mode revealed **11** ($[M + Na]^+$ = 946.6), a dehydrated form of **11** ($[M- H_2O + H]^+$ = 906.6), and a putative octene lactol derivative ($[M + Na]^+$ = 743.6).

Figure S7

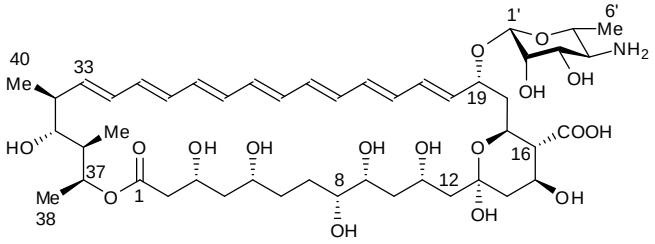

δ_H(500.1 MHz; d^6-DMSO) 0.94 (3 H, d, *J* 6.8, 39-H), 1.06 (3 H, d, *J* 5.9, 40-H), 1.13 (1 H, m, 14b-H)
1.14 (3 H, d, *J* 6.4, 38-H), 1.24 (3 H, d, *J* 6.1, 6′-H), 1.24 and 1.26 (6-H and 7-H), 1.36 (1 H, m, 10b-H),
1.34 (1 H, m, 4b-H), 1.41 (1 H, m, 4a-H), 1.56 (1 H, m, 10a-H), 1.57 (6-H and 7-H),
1.57 (1 H, m, 12b-H), 1.59 (1 H, m, 12a-H), 1.62 (1 H, m, 18b-H), 1.76 (1 H, *ca* ddq, 36-H),
1.91 (1 H, dd, *J* 12.3, 4.6, 14a-H),
1.98 (1 H, m, 18a-H), 2.01 (1 H, *ca* t, *J* 10.3, 16-H), 2.205 and 2.215 (2 H, ABX, 2ab-H),
2.31 (1 H, m, 34-H), 2.81 (1 H, *ca* t, *J* 9.5, 4′-H), 3.12 (1 H, m, 35-H), 3.14 (1 H, m, 8-H),
3.37 (1 H, *ca* dq, *J* 10 and 6.1, 5′-H), 3.44 (1 H, m, 3′-H), 3.47 (1 H, m, 9-H),
3.57 (1 H, m, 5-H), 3.70 (1 H, d, *J* 2.7, 2′-H), 4.05 (1 H, m, 15-H), 4.07 (1 H, m, 3-H),
4.23 (1 H, m, 17-H), 4.24 (1 H, m, 11-H), 4.35 (1 H, br s, 1′-H), 4.40 (1 H, m, 19-H),
5.21 (1 H, dq, *J* 6.8, 2.9, 37-H), 5.45 (1 H, dd, *J* 14.7, 9.7, 33-H),
5.96 (1 H, dd, *J* 15.3 and 8.6, 20-H), 6.10 (1 H, m, 32-H), 6.12 (1 H, m, 21-H), 6.17-6.20 (2 H, m),
6.27 (1 H, dd, *J* 14.8 and 11.0), 6.28-6.37 (5 H, m), 6.40 (1 H, dd, *J* 14.4 and 10.5, 22-H),
6.45 (1 H, dd, *J* 14.5 and 10.8), 7.85 (br s, NH).

Figure S7. (Related to Figure 5) NMR data for perosaminyl-amphoteronolide B (**11**). Data were recorded at 323K (50°C) in d^6-DMSO with HCOOH (1-2 eq) added. Some assignments such as 6-H and 7-H were made by analogy with amphotericin B.

Figure S8

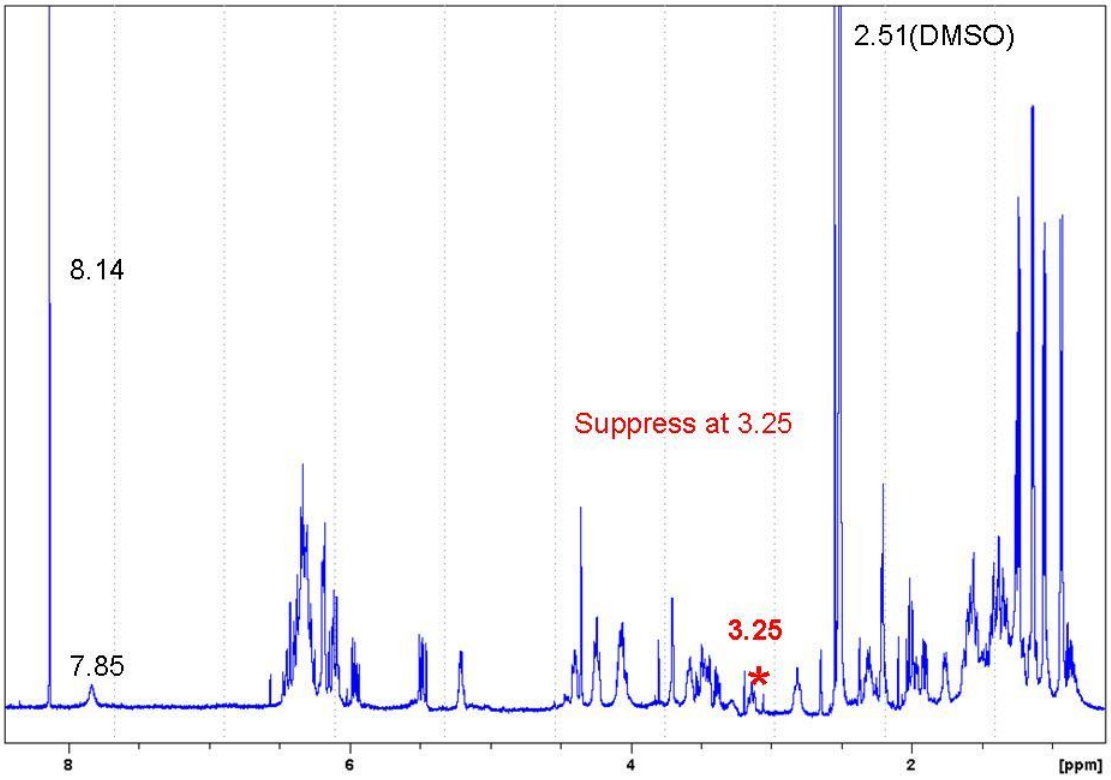

Figure S8. (Related to Figure 5). 500 MHz NMR spectrum of **11**. The spectrum was recorded in d^6-DMSO at 323K with added HCOOH (1-2 eq), and water suppression at 3.25.